Steepest-entropy-ascent quantum thermodynamic modeling of the relaxation process of isolated chemically reactive systems using density of states and the concept of hypoequilibrium state

Guanchen Li* and Michael R. von Spakovsky†
Center for Energy Systems Research, Mechanical Engineering Department, Virginia Tech, Blacksburg, Virginia 24061
(Received 21 April 2015; revised manuscript received 10 September 2015; published 22 January 2016)

This paper presents a study of the nonequilibrium relaxation process of chemically reactive systems using steepest-entropy-ascent quantum thermodynamics (SEAQT). The trajectory of the chemical reaction, i.e., the accessible intermediate states, is predicted and discussed. The prediction is made using a thermodynamic-ensemble approach, which does not require detailed information about the particle mechanics involved (e.g., the collision of particles). Instead, modeling the kinetics and dynamics of the relaxation process is based on the principle of steepest-entropy ascent (SEA) or maximum-entropy production, which suggests a constrained gradient dynamics in state space. The SEAQT framework is based on general definitions for energy and entropy and at least theoretically enables the prediction of the nonequilibrium relaxation of system state at all temporal and spatial scales. However, to make this not just theoretically but computationally possible, the concept of density of states is introduced to simplify the application of the relaxation model, which in effect extends the application of the SEAQT framework even to infinite energy eigenlevel systems. The energy eigenstructure of the reactive system considered here consists of an extremely large number of such levels (on the order of 10^{130}) and yields to the quasicontinuous assumption. The principle of SEA results in a unique trajectory of system thermodynamic state evolution in Hilbert space in the nonequilibrium realm, even far from equilibrium. To describe this trajectory, the concepts of subsystem hypoequilibrium state and temperature are introduced and used to characterize each system-level, nonequilibrium state. This definition of temperature is fundamental rather than phenomenological and is a generalization of the temperature defined at stable equilibrium. In addition, to deal with the large number of energy eigenlevels, the equation of motion is formulated on the basis of the density of states and a set of associated degeneracies. Their significance for the nonequilibrium evolution of system state is discussed. For the application presented, the numerical method used is described and is based on the density of states, which is specifically developed to solve the SEAQT equation of motion. Results for different kinds of initial nonequilibrium conditions, i.e., those for gamma and Maxwellian distributions, are studied. The advantage of the concept of hypoequilibrium state in studying nonequilibrium trajectories is discussed.

DOI: 10.1103/PhysRevE.93.012137

I. INTRODUCTION

There are many modeling approaches in nonequilibrium thermodynamics. From a practical standpoint, models developed from any one of these is typically applicable to a given set of spatial and temporal scales so that in the vein of Grmela and Öttinger [1,2], each model can be classified as being either more macroscopic or less microscopic (or vice versa). Thus, when the nonequilibrium phenomena studied cross different spatial and temporal scales, some form of multiscale model must be employed. This is typically done via multiscale computational techniques, which are able to pass system properties from one scale to another [3–5]. For example, parameters or phenomenological coefficients used in a more macroscopic model are calculated via a more microscopic model, and feedback is used to update them after a time (or distance) interval that is between the characteristic time (or distance) length of the two different models. Such multiscale approaches, nonetheless, present a number of significant drawbacks, not the least of which are computational.

Of course, a general rigorous theoretical framework that permits the study of irreversible phenomena across spatial and temporal scales is of great significance. Two such frameworks exist. The first developed by Grmela and Öttinger [1,2] provides a general equation for nonequilibrium reversible-irreversible coupling (GENERIC) able to couple models from two different scales or levels, i.e., one more microscopic (a level 1 model) and the other more macroscopic (a level 2 model). In general, level 2 models are simpler and rely more on observation and phenomenological descriptions, while those at level 1 are more fundamental and require a significantly higher level of complexity. Grmela and Öttinger suggest that a specific GENERIC equation of motion, which is based on models from two different levels of description, should take the form that satisfies the compatibility of the two models. The analysis of this compatibility, i.e., the passing from a more to a less detailed level, involves a pattern recognition process [1,2], which corresponds to a kind of coarse graining [6,7] that results in what looks like dissipation even if the level 1 dynamics is reversible as in fact they are in mechanics. In this way, the two models and levels are linked via a single equation of motion. Clearly, this approach is more rigorous and fundamental than the multiscale computational technique described earlier. It allows the study of the far-from-equilibrium realm where near-equilibrium parameters no longer hold and the link between two different scale models ensures the compatibility of the two levels in a way that simple parameter delivery cannot.

The second general, rigorous, theoretical framework is that developed by Beretta [6,8–11], which provides a general nonequilibrium dynamics for relaxation crossing different scales. Unlike GENERIC, which bases its approach on

*guanchen@vt.edu
†vonspako@vt.edu

the linking of models across scales into a single equation of motion, Beretta explains irreversible phenomena at different scales using a single thermodynamic model and a single equation of motion, doing so on the basis of the general principle of steepest-entropy ascent (SEA) [8,9,12] or equivalently maximum-entropy production (MEP) (e.g., [13]). In this framework, the irreversible part of the equation of motion is built on a geometrical explanation of relaxation, which results in a gradient dynamics of entropy in state space constrained by the energy, particle number, etc. Since thermodynamic rules and the properties used (specifically, extensive thermodynamic properties such as the energy and the entropy) are applicable across all spatial and temporal scales [14,15], the equation of motion of SEA is well defined and rigorous at all scales. In addition, in Ref. [6], Beretta demonstrates that all of the well-known classical and quantum nonequilibrium frameworks can be formulated within his more general nonequilibrium thermodynamic SEA framework, which is applicable even far from equilibrium.

Although the GENERIC and SEA frameworks approach nonequilibrium thermodynamics from different viewpoints, Montefusco, Consonni, and Beretta [16] show that the dissipative components of the two theories are closely related and in some cases essentially mathematically equivalent, provided that the choice of kinematics is the same, i.e., that both have a common starting point. Furthermore, both provide a geometrical foundation for their dynamics [6,17]. However, differences exist since the SEA framework is a local theory, which starts from local balance equations and implements the principle of maximum local entropy generation compatible with the local conservation constraints, while the GENERIC framework is global, implementing an entropy gradient dynamics compatible with the global conservation constraints.

To date, the SEA framework, which extends a first principles thermodynamic and ensemble representation into the nonequilibrium realm, even that far from equilibrium, has successfully been applied to very microscopic systems such as the state evolution of quantum systems (e.g., [18–23]) as well as to a single-particle classical system [24] whose available microstates are uniformly distributed in phase space. However, its application to high-dimensional state spaces and, thus, to infinite energy eigenlevel (i.e., more macroscopic) systems has necessarily been limited.

To address this limitation, the GENERIC concept of patterns is used here. To begin with, one may view the irreversible term in the SEA framework as resulting from a pattern in a more microscopic model. In a manner similar to the way at stable equilibrium one can view the "Maxwellian distribution" as an invariant pattern even though the mechanical details of the individual particle states constantly change, steepest-entropy ascent can also be viewed as a changing global pattern or effect of the details of the mechanics in relaxation. Thus, without including all of the details of the more microscopic model (i.e., of the mechanics), the pattern of this model serves as a modification of the more macroscopic model (i.e., of the nonequilibrium thermodynamics). This, of course, greatly simplifies the computational complexity, while the clear physical meaning and geometrical description of the SEA landscape facilitates the discovery of general but unique patterns of relaxation in the nonequilibrium realm at any scale.

In view of this, two nonequilibrium relaxation patterns present themselves, which offer two methods for practically (i.e., computationally) extending the application of the steepest-entropy-ascent quantum thermodynamics (SEAQT) framework to infinite-dimensional state spaces, even those in the macroscopic continuous spectrum, and for extending an equilibrium-type description to nonequilibrium states. This extension focuses on the irreversible process of thermodynamic mixture states in which the Hamiltonian dynamics vanishes and the state evolution is due only to thermodynamic irreversibilities. Both methods originate from physical concepts. The discussion begins in Sec. II with a brief description of the SEAQT framework and focuses on the trajectory of system thermodynamic state evolution and not its time evolution since it is the trajectory which reveals the geometric features of interest. The concept of hypoequilibrium state is then introduced, which permits temperature to be defined for all nonequilibrium states and implies that the energy eigenlevels in mutual equilibrium evolve as a group. This is followed in Sec. III by a description of our density of state method, which allows the macroscopic-level SEAQT equation of motion to be solved. It is based on the idea that similar eigenlevels with similar initial conditions evolve similarly. Finally, in Sec. IV, the thermodynamic-ensemble based approach developed and presented in the previous sections is applied within the SEAQT framework to the study of an isolated, chemically reactive, macroscopic system undergoing a nonequilibrium evolution in state. This approach, in fact, represents a computationally simpler, alternative global method for predicting the chemical kinetics of systems, even those far from equilibrium, and does so without the need for the detailed particle mechanics (e.g., that of particle collisions) of conventional approaches or for such limiting assumptions as local or global equilibrium. Topics illustrated and discussed include the features of the nonequilibrium trajectories predicted, the density of states of the chemical reaction process, and the influence of the initial nonequilibrium states on the trajectories. Two generalizations to the nonequilibrium realm of stable equilibrium concepts are also physically illustrated and discussed, i.e., that of hypoequilibrium state and that of nonequilibrium temperature. The former leads to the definition of the latter and to the possibility of representing a very large class of nonequilibrium states and of approximating an even larger class of other nonequilibrium states in the study of nonequilibrium trajectories.

II. THEORY: STEEPEST-ENTROPY-ASCENT EQUATION OF MOTION

A. Nonequilibrium evolution framework

Based on the discussion by Grmela [1,2,17] and Beretta [6,16], the general form of a nonequilibrium framework is a combination of both irreversible relaxation and reversible symplectic dynamics. If written in a generalized form of the Ginzburg-Landau equation [1,16], the equation of motion takes the following form:

$$\frac{d}{dt}\alpha(t) = X^H_{\alpha(t)} + Y^H_{\alpha(t)}, \tag{1}$$

where $\alpha(t)$ represents the state evolution trajectory, $X^H_{\alpha(t)}$ and $Y^H_{\alpha(t)}$ are functions of the system state $\alpha(t)$ and represent

the reversible symplectic dynamics and irreversible relaxation process, respectively. In the SEAQT framework, the system state is represented by the density operator $\hat{\rho}$, $X^H_{\alpha(t)}$ follows the Schrödinger equation, and $Y^H_{\alpha(t)}$ is derived from the SEA principle. Thus,

$$\frac{d\hat{\rho}}{dt} = \frac{1}{i\hbar}[\hat{\rho},\hat{H}] + \frac{1}{\tau(\hat{\rho})}\hat{D}(\hat{\rho}). \tag{2}$$

$\hat{D}$ is the dissipation operator determined via a constrained gradient in Hilbert space. A metric tensor must be specified in the derivation of this dissipation term since it describes the geometric features of the Hilbert space [6]. τ is the relaxation time, which represents the speed of system evolution in Hilbert space. A general discussion of the SEA formulation of dissipation, using other forms of metric and symplectic terms, is given in Ref. [6] with examples of five nonequilibrium thermodynamic frameworks. Furthermore, a version of Eq. (2) for a general quantum system is used in Ref. [21] to predict and compare with experimental results the decorrelation and decoherence of a system in which the Schrödinger dynamics and relaxation process are coupled. In this paper, the version of Eq. (2) considered is for the case when the symplectic part vanishes and only the relaxation part remains. For this case, the SEA equation of motion exhibits useful mathematical features (e.g., hypoequilibrium states) that enable a clear physical representation of nonequilibrium state evolution and lead to a fast and accurate computational solution.

An example of such an evolution, i.e., that of a pure relaxation process, is the application here of the SEAQT framework to the modeling of an isolated chemically reactive system. The system is restricted to the class of dilute-Boltzmann-gas states in which the particles are independently distributed [10]. Such states can be represented by a single-particle density operator that is diagonal in the basis of the single-particle eigenstates. In addition, the Hilbert space metric chosen is the Fisher-Rao metric, which is uniform in different dimensions of Hilbert space. Under these conditions, the symplectic Schrödinger term in the equation of motion vanishes, and the study is able to focus on the irreversible relaxation process only.

B. System and state

Sections II B and II C provide a brief introduction to the SEA equation of motion for dilute Boltzmann gases. More details can be found in Refs. [10,25]. The system studied has the Hamiltonian H, and the eigenvalues and eigenvectors of the corresponding operator $\hat{H}$ take the form

$$\hat{H}|\phi_k\rangle = \epsilon_k|\phi_k\rangle, \quad k = 1,2,\ldots \tag{3}$$

where k is the index for the energy eigenlevels. Degeneracy in which an energy eigenlevel can have the same eigenvalue with different eigenvectors is allowed. Equivalently, the system can also be defined by a group of energy eigenlevels and eigenvectors such that

$$\hat{H} = \sum_k \epsilon_k|\phi_k\rangle\langle\phi_k|. \tag{4}$$

The thermodynamic state of the system can be defined via a probability distribution $\{p_k\}$ among the energy eigenlevels $\{\epsilon_k\}$, which accounts for the diagonal term of the density operator. An element of $\{\epsilon_k\}$ can share the same value in case of degeneracy. As an example, the stable equilibrium state of the system has the following canonical distribution, which provides the maximum entropy:

$$p_k = \frac{1}{Z}e^{-\frac{\epsilon_k}{k_bT}}, \tag{5}$$

where Z is the partition function $Z = \sum e^{-\frac{\epsilon_k}{k_bT}}$ and the equilibrium temperature is T. Any other state, represented by a probability distribution other than the canonical distribution, is a nonequilibrium state since the entropy is not a maximum.

The probability space $\{p_k\}$ is the state space for the system. The statistical distance dl between $p_k(\theta)$ and $p_k(\theta + d\theta)$ can be defined by the Fisher-Rao metric such that

$$dl = \frac{1}{2}\sqrt{\sum_k p_k\left(\frac{d\ln p_k}{d\theta}\right)^2}\,d\theta. \tag{6}$$

More discussion on choosing a metric can be found in Ref. [6]. The parameter θ is continuous and can be chosen as the time t. Now, in order to simplify the representation of the development of the equation of motion in the next two sections (Secs. II B and II C), the square root of the probability $x_i = \sqrt{p_i}$ is defined so that the probability space can be represented by $\boldsymbol{x} = \{x_i\}$. The statistical distance then takes the form

$$dl = \frac{1}{2}\sqrt{\sum_k \frac{1}{p_k}\left(\frac{dp_k}{d\theta}\right)^2}\,d\theta = \sqrt{\sum_k (dx_k)^2}, \tag{7}$$

where the distance between any two distributions $\boldsymbol{x^a}$ and $\boldsymbol{x^b}$ is the angle

$$d(\boldsymbol{x^a},\boldsymbol{x^b}) = \cos^{-1}\left(\sum_k x^a_k x^b_k\right) = \cos^{-1}(\boldsymbol{x^a}\cdot\boldsymbol{x^b}). \tag{8}$$

According to the discussion in Ref. [26], this statistical distance is equivalent to an angle in Hilbert space and has a precise physical meaning in quantum mechanics. Thus, the state of the system as well as the distance in state space can be represented by $\boldsymbol{x}$ and $dl^2 = \sum_k (dx_k)^2 = d\boldsymbol{x}\cdot d\boldsymbol{x}$.

Now, if time t is chosen as the parameter, from Eq. (7) one can arrive at

$$\frac{dl}{dt} = \sqrt{\sum_k \left(\frac{dx_k}{dt}\right)^2}, \tag{9}$$

which is the speed of the motion in probability or state space.

C. Property and the equation of motion

A property of the system can be defined as a function of state $\{x_k\}$ such that

$$I = \sum_k x_k^2, \tag{10}$$

$$E = \langle e\rangle = \sum_k \epsilon_k x_k^2, \tag{11}$$

$$S = \langle s\rangle = \sum_k -x_k^2\ln\left(x_k^2\right), \tag{12}$$

where $\langle \ldots \rangle$ means the ensemble average. The von Neumann formula for entropy is used because, as shown in Ref. [14], it has all the characteristics required by thermodynamics.

The gradient of a given property in state space is then expressed by

$$\boldsymbol{g_I} = \sum_k \frac{\partial I}{\partial x_k}\hat{e_k} = \sum_k 2x_k\hat{e_k}, \tag{13}$$

$$\boldsymbol{g_E} = \sum_k \frac{\partial E}{\partial x_k}\hat{e_k} = \sum_k 2\epsilon_k x_k\hat{e_k}, \tag{14}$$

$$\boldsymbol{g_S} = \sum_k \frac{\partial S}{\partial x_k}\hat{e_k} = \sum_k \left[-2x_k - 2x_k \ln\left(x_k^2\right)\right]\hat{e_k}, \tag{15}$$

where $\hat{e_k}$ is the unit vector for each dimension. Furthermore, for an isolated system, the system satisfies the conservation laws for probability and energy, i.e.,

$$I = \sum_k x_k^2 = 1, \tag{16}$$

$$E = \sum_k \epsilon_k x_k^2 = \text{constant} \tag{17}$$

and the principle of SEA upon which the equation of motion is based is defined as the system state evolving along the direction that at any instant of time has the largest entropy gradient consistent with the conservation constraints. Since the reversible term vanishes for dilute Boltzmann gases in an isolated system, the equation of motion for the irreversible relaxation process is given by

$$\frac{d\boldsymbol{x}}{dt} = \frac{1}{4\tau(x)}\boldsymbol{g_{S\perp L(g_I,g_E)}}, \tag{18}$$

where τ, which is a function of system state, is the relaxation time that describes the speed at which the state evolves in state space in the direction of steepest-entropy ascent. $L(\boldsymbol{g_I},\boldsymbol{g_E})$ is the manifold spanned by $\boldsymbol{g_I}$ and $\boldsymbol{g_E}$, and $\boldsymbol{g_{S\perp L(g_I,g_E)}}$, which lies parallel to the hypersurface that conserves the probability and the energy, is the perpendicular component of the gradient of the entropy to the manifold $L(\boldsymbol{g_I},\boldsymbol{g_E})$. It takes the form of a ratio of Gram determinants such that

$$\boldsymbol{g_{S\perp L(g_I,g_E)}} = \frac{\begin{vmatrix} \boldsymbol{g_S} & \boldsymbol{g_I} & \boldsymbol{g_E} \\ (\boldsymbol{g_S},\boldsymbol{g_I}) & (\boldsymbol{g_I},\boldsymbol{g_I}) & (\boldsymbol{g_E},\boldsymbol{g_I}) \\ (\boldsymbol{g_S},\boldsymbol{g_E}) & (\boldsymbol{g_I},\boldsymbol{g_E}) & (\boldsymbol{g_E},\boldsymbol{g_E}) \end{vmatrix}}{\begin{vmatrix} (\boldsymbol{g_I},\boldsymbol{g_I}) & (\boldsymbol{g_E},\boldsymbol{g_I}) \\ (\boldsymbol{g_I},\boldsymbol{g_E}) & (\boldsymbol{g_E},\boldsymbol{g_E}) \end{vmatrix}}, \tag{19}$$

where $(\ldots,\ldots)$ denotes the scalar product of two vectors in state space. The explicit form of Eq. (18) for $\{x_k\}$ is, thus,

$$\frac{dx_k^2}{dt} = \frac{1}{\tau}\frac{\begin{vmatrix} -x_k^2\ln x_k^2 & x_k^2 & \epsilon_k x_k^2 \\ \langle s\rangle & 1 & \langle e\rangle \\ \langle es\rangle & \langle e\rangle & \langle e^2\rangle \end{vmatrix}}{\begin{vmatrix} 1 & \langle e\rangle \\ \langle e\rangle & \langle e^2\rangle \end{vmatrix}} \tag{20}$$

and for $\{p_k\}$ [10]

$$\frac{dp_k}{dt} = \frac{1}{\tau}\frac{\begin{vmatrix} -p_k\ln p_k & p_k & \epsilon_k p_k \\ \langle s\rangle & 1 & \langle e\rangle \\ \langle es\rangle & \langle e\rangle & \langle e^2\rangle \end{vmatrix}}{\begin{vmatrix} 1 & \langle e\rangle \\ \langle e\rangle & \langle e^2\rangle \end{vmatrix}}. \tag{21}$$

D. Equation of motion with degeneracy

The energy eigenlevels $\{\epsilon_k,\ k = 1,2,\ldots\}$ and $\{|\phi_k\rangle,\ k = 1,2,\ldots\}$ can be reordered and grouped into $\{\epsilon_{ij},\ i = 1,2,\ldots,\ \ j = 1,\ldots,n_i\}$ and $\{|\phi_{ij}\rangle,\ \ i = 1,2,\ldots,\ \ j = 1,\ldots,n_i\}$, where $\{\epsilon_{ij} = \epsilon_i,\ \ j = 1,\ldots,n_i\}$ are degenerate energy eigenlevels with degeneracy n_i. For the equation of motion (21), the degenerate eigenstates for a given eigenvalue with the same initial probability are equivalent, and have the same occupation probabilities at all times, which means $p_{ij} = p_{ik}$ for any j,k. For example, the initial distribution among these eigenlevels is proportional to the canonical distribution that gives equal initial probabilities for each degenerate eigenstate. This is the case when these eigenlevels come from the same subsystem of a system in a hypoequilibrium state (see Sec. II F). Thus, without loss of generality, the degenerate energy eigenlevels with the same initial probabilities can be combined, and the energy eigenlevels represented by the monotonically nondecreasing energy eigenvalue series $\{\tilde{\epsilon}_i\}$ with degeneracy $\{n_i\}$. The probability $\{\tilde{p}_i\}$ at energy eigenlevel $\{\tilde{\epsilon}_i\}$ is given by

$$\tilde{p}_i = \tilde{x}_i^2 = \sum_{j=1}^{n_i} x_{ij}^2, \tag{22}$$

$$x_{ij}^2 = \frac{1}{n_i}\tilde{p}_i = \frac{1}{n_i}\tilde{x}_i^2. \tag{23}$$

The system state can, therefore, be represented by a new vector $\{\tilde{x}_i\}$ or $\{\tilde{p}_i\}$ in a new probability space formed by the probability distribution among the energy eigenlevels $\{\tilde{\epsilon}_i\}$. The equality of statistical distance in the original probability space with that in the new probability space is shown by the following development:

$$dl^2 = \sum_i\sum_{j=1}^{n_i}(dx_{ij})^2 = \sum_i\sum_{j=1}^{n_i}\left(\frac{1}{\sqrt{n_i}}d\tilde{x}_i\right)^2 = \sum_i(d\tilde{x}_i)^2, \tag{24}$$

$$\begin{aligned} d(\boldsymbol{x^a},\boldsymbol{x^b}) &= \cos^{-1}\left(\sum_i\sum_{j=1}^{n_i}x_{ij}^a x_{ij}^b\right) \\ &= \cos^{-1}\left(\sum_i\sum_{j=1}^{n_i}\frac{1}{\sqrt{n_i}}\tilde{x}_i^a\frac{1}{\sqrt{n_i}}\tilde{x}_i^b\right) \\ &= \cos^{-1}\left(\sum_i\tilde{x}_i^a\tilde{x}_i^b\right) = d(\tilde{\boldsymbol{x}}^{\boldsymbol{a}},\tilde{\boldsymbol{x}}^{\boldsymbol{b}}). \end{aligned} \tag{25}$$

In this new vector space, system properties such as I, E, and S are expressed as

$$I = \sum_i \tilde{x}_i^2, \tag{26}$$

$$E = \langle e \rangle = \sum_i \tilde{\epsilon}_i \tilde{x}_i^2, \tag{27}$$

$$S = \langle s \rangle = \sum_i -\tilde{x}_i^2 \ln\left(\frac{\tilde{x}_i^2}{n_i}\right), \tag{28}$$

while the equation of motion changes to the following forms for $\{\tilde{x}_j\}$ and $\{\tilde{p}_j\}$:

$$\frac{d\tilde{x}_j^2}{dt} = \frac{1}{\tau}\frac{\begin{vmatrix} -\tilde{x}_j^2 \ln \frac{\tilde{x}_j^2}{n_j} & \tilde{p}_j & \epsilon_j \tilde{x}_j^2 \\ \langle s \rangle & 1 & \langle e \rangle \\ \langle es \rangle & \langle e \rangle & \langle e^2 \rangle \end{vmatrix}}{\begin{vmatrix} 1 & \langle e \rangle \\ \langle e \rangle & \langle e^2 \rangle \end{vmatrix}}, \tag{29}$$

$$\frac{d\tilde{p}_j}{dt} = \frac{1}{\tau}\frac{\begin{vmatrix} -\tilde{p}_j \ln \frac{\tilde{p}_j}{n_j} & \tilde{p}_j & \epsilon_j \tilde{p}_j \\ \langle s \rangle & 1 & \langle e \rangle \\ \langle es \rangle & \langle e \rangle & \langle e^2 \rangle \end{vmatrix}}{\begin{vmatrix} 1 & \langle e \rangle \\ \langle e \rangle & \langle e^2 \rangle \end{vmatrix}}. \tag{30}$$

This new equation of motion for degenerate energy eigenlevels is a simplification of the equation of motion of Sec. II C for the assumption that $p_{ij} = p_{ik}$ for any j,k. Equations (24)–(30) are acquired by substituting Eq. (22) into Eqs. (7), (8), (10)–(12), (20), and (21). Since the discussions in the next sections are based on Eq. (30), the tilde used to designate the probabilities of the new probability space are dropped for simplicity.

E. Nonequilibrium evolution trajectory: Kinetics versus dynamics

In this section, the kinetics and dynamics of nonequilibrium state evolution are introduced. The result of this section applies to a system with a relaxation process only (i.e., without a symplectic term in the equation of motion) but is not limited to a Fisher-Rao metric system. The equation of motion for a degenerate system [Eq. (30)] is first simplified by defining A_1, A_2, and A_3 such that

$$A_1 = \begin{vmatrix} 1 & \langle e \rangle \\ \langle e \rangle & \langle e^2 \rangle \end{vmatrix}, \quad A_2 = \begin{vmatrix} \langle s \rangle & \langle e \rangle \\ \langle es \rangle & \langle e^2 \rangle \end{vmatrix}, \quad A_3 = \begin{vmatrix} \langle s \rangle & 1 \\ \langle es \rangle & \langle e \rangle \end{vmatrix}. \tag{31}$$

The equation of motion then becomes

$$\frac{dp_j}{dt} = \frac{1}{\tau}\left(-p_j \ln \frac{p_j}{n_j} - p_j \frac{A_2}{A_1} + \epsilon_j p_j \frac{A_3}{A_1}\right). \tag{32}$$

The solution of this equation is

$$p_j = p_j(t), \tag{33}$$

where the time evolution of the probability can be regarded as a parametric equation with parameter t. If t is the real time, the solution of Eq. (32) provides both the trajectory in state space and the system state at any instant of time.

In general, the relaxation time τ can be a function of system state such that

$$\tau = \tau[\boldsymbol{p}(t)] \tag{34}$$

since for a given initial state of the system, the nonequilibrium path of state evolution is uniquely obtained from the equation of motion (32). This path can be used to define a new parameter $\tilde{\tau}$ given by

$$d\tilde{\tau} = \frac{1}{\tau[\boldsymbol{p}(t)]}dt \quad \text{or} \quad \tilde{\tau} = \int_{\text{path}} \frac{1}{\tau[\boldsymbol{p}(t')]}dt' = \tilde{\tau}(t), \tag{35}$$

where $\tilde{\tau}$ is called the dimensionless time. With this time, the independent variable for the equation of motion can be changed so that

$$\frac{dp_j}{d\tilde{\tau}} = -p_j \ln \frac{p_j}{n_j} - p_j \frac{A_2}{A_1} + \epsilon_j p_j \frac{A_3}{A_1}. \tag{36}$$

The solution for this equation is written as

$$p_j = p_j(\tilde{\tau}). \tag{37}$$

No matter how the relaxation time τ depends on the real time t and the state, the equation of motion can always be transformed into Eq. (36) with the parameter change defined by Eq. (35). Furthermore, the evolution of system state follows the same function [Eq. (37)] in $\tilde{\tau}$. Physically, this means that the system follows the same trajectory in state space, while τ decides the speed with which the system's state moves along the trajectory. If the relaxation time is chosen to be a constant, Eq. (33) gives the same parametric equation [Eq. (37)] with a parametric scaling in the relaxation time τ. Thus, the kinetics and dynamics of the system are separated. The former are found via Eqs. (36) and (37) and result in the trajectory in state space based on the parameter $\tilde{\tau}$ or a constant relaxation time τ. The dynamics is found via Eq. (32) and the functional dependence $\tau = \tau(\boldsymbol{p})$ [Eq. (34)] and result in the trajectory in state space based on the real time t. Recent numerical results show that a uniform (Fisher-Rao) metric may for some systems provide poor performance relative to the time evolution [24] at least in the near-equilibrium limit. In such cases, the time evolution needs more information on the dynamics or the function τ. For this reason, the results presented here are restricted to the kinetic evolution trajectory and the intermediate states of the relaxation process, and, thus, to the purely geometrical features of the relaxation process.

F. Description of the trajectory: Subsystem hypoequilibrium state and temperature

In this section, the concepts of subsystem hypoequilibrium state and temperature for a system in a nonequilibrium state are defined. These two concepts support the physical description of the evolution trajectory in state space rather than just its mathematical description. However, this description is restricted to systems with irreversible relaxations only. These concepts originate from a generalization of the canonical distribution to a nonequilibrium distribution in Hilbert space with a uniform metric (Fisher-Rao metric). However, such a generalization under any metric is an open question. Furthermore, to be general, the relaxation time in this section can be constant or a function of system state, which means that the conclusions drawn apply to both the kinetic and dynamic characteristics of the state space trajectory.

For a given system represented by an energy eigenlevel set $\Omega = \{\epsilon_k\}$, the system can be divided into M subsystems (i.e., subspaces in state space) $\Omega_i = \{\epsilon_{ik}\}$, $\Omega = \cup\, \Omega_i$, and $\Omega_i \cap \Omega_j = \emptyset$ for any $i, j = 1, \ldots, M$. If the probability distribution

in each subsystem yields to a canonical distribution, the system is designated as being in an Mth-order hypoequilibrium state. Based on this definition, any state of the system (strictly speaking, a diagonal density operator in an eigenstate basis) is a hypoequilibrium state with order M, where M is less than or equal to the number of system eigenlevels. A hypoequilibrium state of order 1 corresponds to a state in stable equilibrium. The probability distribution of the Mth-order hypoequilibrium state takes the form

$$\forall\, i = 1,2,\ldots,M, \quad p_{ik} = \alpha_i n_{ik} e^{-\beta_i \epsilon_{ik}}, \quad k = 1,2,\ldots,w_i \tag{38}$$

where α_i and β_i are parameters, and n_{ik} is the degeneracy of ϵ_{ik}. To be complete, $\beta_i = 0$ if $w_i = 1$, and w_i can be infinite.

$\alpha_i Z_i(\beta_i)$ has the physical meaning of particle number where Z_i is the partition function of the subsystem. The inverse of the temperature of each subsystem Ω_i is β_i with a scale of the Boltzmann constant. This temperature is defined for each subsystem when the system is in a state of nonequilibrium. It is proven in the following that if a system begins in an Mth-order hypoequilibrium state, it will remain in an Mth-order hypoequilibrium state throughout the time evolution as will the subsystem division. To show this, Eq. (32) is reformulated such that

$$\frac{d}{dt}\ln\frac{p_j}{n_j} = \frac{1}{\tau}\left(-\ln\frac{p_j}{n_j} - \frac{A_2}{A_1} + \epsilon_j\frac{A_3}{A_1}\right), \tag{39}$$

where it is noted that $d(\ln n_j)/dt$ is zero and that A_1, A_2, and A_3 are the same for all chosen energy eigenlevels p_j and only a function of the entire probability distribution at a given instant of time. Subtracting the equations of motion for the ith and kth energy eigenlevels results in

$$\frac{d}{dt}\left(\ln\frac{p_j}{n_j} - \ln\frac{p_k}{n_k}\right) = -\frac{1}{\tau}\left(\ln\frac{p_j}{n_j} - \ln\frac{p_k}{n_k}\right) + \frac{1}{\tau}\frac{A_3}{A_1}(\epsilon_j - \epsilon_k). \tag{40}$$

Defining a new variable

$$W_{jk} = \frac{1}{\epsilon_j - \epsilon_k}\left(\ln\frac{p_j}{n_j} - \ln\frac{p_k}{n_k}\right), \tag{41}$$

the time evolution of W_{jk} yields to the ordinary differential equation

$$\frac{dx}{dt} = -\frac{1}{\tau}x + \frac{1}{\tau}\frac{A_3}{A_1}. \tag{42}$$

If p_j and p_k are in the same subsystem for which the initial probability distribution is a canonical one, i.e., if

$$p_j(t=0) = \alpha_p n_j e^{-\epsilon_j\beta_p}, \quad p_k(t=0) = \alpha_p n_k e^{-\epsilon_k\beta_p}, \tag{43}$$

then

$$W_{jk}(t=0) = \frac{1}{\epsilon_j - \epsilon_k}\left(\ln\frac{p_j}{n_j} - \ln\frac{p_k}{n_k}\right) = -\beta_p. \tag{44}$$

For $\forall\ p_j, p_k$ in the same subsystem Ω_p, the time evolution of W_{jk} yields to the same ordinary differential equation (ODE) with the same initial value, namely,

$$\frac{dx}{dt} = -\frac{1}{\tau}x + \frac{1}{\tau}\frac{A_3}{A_1}, \quad x = W_{jk}(t=0) = -\beta_p \tag{45}$$

so that the solution of W_{jk} is the same $W_{jk}(t) = \beta_p(t)$. Therefore, the probability distribution in this subsystem maintains the canonical distribution with the parameter $\beta_p(t)$ given by

$$p_j(t) = \alpha_p(t) n_j e^{-\epsilon_j\beta_p(t)}. \tag{46}$$

In addition, the temperature of the subsystem at time t is defined by

$$T_p(t) = \frac{1}{k_b\beta_p(t)}. \tag{47}$$

Thus, for a system in a nonequilibrium state, the hypoequilibrium temperature for each subsystem is defined. This temperature can be the same or different from that of any other subsystem. If a system is in an Mth-order hypoequilibrium state, it remains at least of order M throughout as well as after the evolution, and the probability distribution of each subsystem remains canonical. More discussion on the evolution of temperature is given in Sec. V. In addition, the ODE for β_p [Eq. (45)] is independent of α_p so that different subsystems with the same initial β_p also keep the same $\beta_p(t)$ in the evolution. This phenomenon is consistent with the idea that energy via a heat interaction cannot transfer between systems with the same temperature to produce a temperature difference. Equal temperature subsystems maintain equal temperatures.

Moreover, if two subsystems A and B are in mutual equilibrium at time t_{me} $[\alpha_p(t_{me})^A = \alpha_p(t_{me})^B$, $\beta_p(t_{me})^A = \beta_p(t_{me})^B]$, the combination of these two subsystems yields a subsystem with a canonical distribution. This new subsystem maintains a canonical distribution throughout its state evolution, which means that the two original subsystems maintain their hypoequilibrium states as well as a state of mutual equilibrium with each other.

The results just demonstrated are summarized as follows: (i) the manner of subdividing the system is invariant with respect to the irreversible relaxation trajectory; (ii) the probability distribution in each subsystem remains canonical along the trajectory so that temperature can be defined based on a parameter of the canonical distribution; and (iii) equal temperature subsystems maintain equal temperatures, and subsystems in mutual equilibrium remain in mutual equilibrium. With the concept of subsystem hypoequilibrium state, the trajectory for system state evolution in state space is described by two functions $\alpha_p(t)$ and $\beta_p(t)$. Physically, each instantaneous value of $\alpha_p(t)Z_p[\beta_p(t)]$ is the total probability (particle number) of a given subsystem, while each instantaneous value of $\beta_p(t)$ is the parameter of the canonical distribution and the inverse of the subsystem temperature. $Z_p[\beta(t)]$ is the partition function, which is a function of β. Thus, $\alpha_p(t)$ describes the probability transfer between subsystems, while $\beta_p(t)$ describes the temperature evolution and heat diffusion between subsystems. No longer is the canonical distribution simply a characteristic of stable equilibrium but instead a characteristic of subsystem hypoequilibrium and maximum-entropy generation as well. This feature provides a convenient pattern for studying the evolution of a system's state distribution during an irreversible relaxation process.

For a complete discussion on subspace temperature and a set of general nonequilibrium intensive properties, the reader is referred to [27–29]. Some conclusions from these

references are given in Appendix B, including a clear physical picture, based on the concepts of hypoequilibrium state and nonequilibrium intensive property, of the generalization of the Onsager relations and the dissipation potential to the nonequilibrium realm. In addition, for a discussion of the relationship of the general Onsager framework of nonequilibrium thermodynamics [30] to SEAQT and GENERIC, the reader is referred to [6,25] for the SEAQT framework and to [31] for the GENERIC.

III. MODEL: DENSITY OF STATE METHOD

In this section, the numerical method for solving the SEAQT equation of motion is introduced. Called the density of state method, its purpose is to solve this equation for an extremely large number of energy eigenlevels, a number, in fact, so large that even the state evolution of macroscopic systems can be determined. This numerical method follows the same idea as the derivation of the equation of motion for a degenerate system, namely, that similar eigenlevels with similar initial states evolve similarly. An example of a system with a very large number of levels is that of an ideal gas at a temperature higher than the characteristic temperature for translation. A practical illustration is given in Sec. IV.

A. Probability cut

For an isolated system with unbounded energy, the probability distribution is assumed to be limited to a bounded range of energy eigenlevels. This means that in the $\lim_{K\to\infty} p(\epsilon > \epsilon_K) = 0$, and the energy eigenlevels in the bounded range can be used to approximate the unbounded range of the system. For a given system $\{\epsilon_i,\ i = 1,2,\ldots\}$ and initial state $\{p_i,\ i = 1,2,\ldots\}$, K is chosen such that $\sum_{i>K} p_K < \delta$ resulting in $\epsilon_{\rm cut} = \epsilon_K$ and the set of system bounded energy eigenvalues $\epsilon_i < \epsilon_{\rm cut}$.

B. Evolution of probability in energy intervals

For a system with bounded energy eigenvalues, a subset of the energy eigenlevels can be chosen to be a subsystem or an entire system. The range of energy eigenlevels of this subset is then separated into finite intervals such that

$$\begin{aligned} &e_i = \epsilon_{\rm ground} + \frac{i}{R}(\epsilon_{\rm cut} - \epsilon_{\rm ground}),\\ &\text{Interval: } [e_{i-1},e_i], \quad i = 1,\ldots,R\\ &\text{Interval length: } \Delta E = e_i - e_{i-1}, \quad i = 1,\ldots,R \end{aligned} \tag{48}$$

where R is the number of intervals. Integrating the equation of motion (32) over the ith interval $[e_{i-1},e_i]$ yields the equation of motion for the probability in the ith interval, namely,

$$\frac{dP_i}{dt} = \frac{1}{\tau}\left(\langle s\rangle_i - P_i\frac{A_2}{A_1} + \langle e\rangle_i\frac{A_3}{A_1}\right), \tag{49}$$

where $P_i = \sum_{\epsilon_k\in[e_{i-1},e_i]} p_k$ is the probability distributed over the energy levels in the interval $[e_i,e_{i-1}]$, $\langle s\rangle_i = -\sum_{\epsilon_k\in[e_{i-1},e_i]} p_k \ln(p_k/n_k)$ is the contribution of this energy interval to the total entropy, and $\langle e\rangle_i = \sum_{\epsilon_k\in[e_{i-1},e_i]} \epsilon_k p_k$ is the contribution of this energy interval to the total energy. By summing the property of every energy interval, the property of the whole system (e.g., the total entropy and total energy) can be determined.

C. Energy spectrum agglomeration

For a given initial state, the energy eigenlevels of the system can be separated into M groups. Each group forms a subsystem, and the probability distribution of each subsystem is assumed to be a gamma distribution or its linear combination, which can cover quite a large range of initial conditions. A subsystem K is chosen, and its range of energy eigenvalues divided into R intervals. It is assumed that there are m_i energy eigenvalues $\{\epsilon^i_j,\ j = 1,\ldots,m_i\}$ with degeneracies $\{n^i_j,\ j = 1,\ldots,m_i\}$ in the interval $[e_{i-1},e_i]$ of subsystem K where m_i can be infinity.

A pseudosubsystem with energy eigenvalues $\{E_i,\ i = 1,\ldots,R\}$ and degeneracies $\{N_i,\ i = 1,\ldots,R\}$ is then constructed such that

$$N_i = \sum_{j=1}^{m_i} n^i_j, \tag{50}$$

$$E_i = \frac{1}{N_i}\sum_{j=1}^{m_i} n^i_j\epsilon^i_j. \tag{51}$$

For any distribution, P_i is the distribution of the ith interval of the Kth subsystem expressed by

$$P_i = \sum_{j=1}^{m_i} p^i_j. \tag{52}$$

If the subsystem has a distribution given by

$$p^i_j = Cn^i_j\left(\epsilon^i_j\right)^\theta e^{-\epsilon^i_j\beta}, \tag{53}$$

where C is a constant, n^i_j is the degeneracy of energy eigenlevel ϵ^i_j. The pseudosubsystem distribution at the same temperature is expressed as

$$\hat{P}_i = CN_i(E_i)^\theta e^{-E_i\beta}, \tag{54}$$

where C is the same as in Eq. (53). In Appendix A, $\hat{P}_i$ is proven to be equal to P_i for most energy intervals under the quasicontinuous condition expressed as

$$\frac{1}{\beta} \gg |E_{i+1} - E_i| > \left|\epsilon^i_j - E_i\right|. \tag{55}$$

Note that $\hat{P}_i$ becomes a probability distribution with normalization condition when the system as a whole is considered. It is assumed that the quasicontinuous condition holds both for the pseudosubsystem as well as the original subsystem. Now, for the original subsystem,

$$\langle e\rangle_i = \sum_j p^i_j\epsilon^i_j, \tag{56}$$

$$\langle s\rangle_i = -\sum_j p^i_j \ln\frac{p^i_j}{n^i_j}, \tag{57}$$

$$\langle e\rangle_K = \sum_i\sum_j p^i_j\epsilon^i_j, \tag{58}$$

$$\langle s\rangle_K = -\sum_i \sum_j p_j^i \ln \frac{p_j^i}{n_j^i}, \tag{59}$$

$$\langle es\rangle_K = -\sum_i \sum_j p_j^i \epsilon_j^i \ln \frac{p_j^i}{n_j^i}, \tag{60}$$

$$\langle e^2\rangle_K = \sum_i \sum_j p_j^i \left(\epsilon_j^i\right)^2, \tag{61}$$

while for the pseudosubsystem,

$$\langle \hat{e}\rangle_i = E_i \hat{P}_i, \tag{62}$$

$$\langle \hat{s}\rangle_i = -\hat{P}_i \ln \frac{\hat{P}_i}{N_i}, \tag{63}$$

$$\langle \hat{e}\rangle_K = \sum_i \hat{P}_i E_i, \tag{64}$$

$$\langle \hat{s}\rangle_K = -\sum_i \hat{P}_i \ln \frac{\hat{P}_i}{N_i}, \tag{65}$$

$$\langle \hat{es}\rangle_K = -\sum_i \hat{P}_i E_i \ln \frac{\hat{P}_i}{N_i}, \tag{66}$$

$$\langle \hat{e^2}\rangle_K = \sum_i \hat{P}_i E_i^2. \tag{67}$$

Here, $\langle \ldots\rangle_i$ stands for the contribution of the ith interval of the pseudosubsystem or original subsystem to the system property, while $\langle \ldots\rangle_K$ stands for the contribution of the entire Kth subsystem to the system property. The system properties are then found as is done in Appendix A by summing the subsystem properties over the index K. In Appendix A, it is proven that under the quasicontinuous condition, a pseudosubsystem property in a given energy interval is in most cases equal to that of the original subsystem, and the associated subsystem and system property as well as A_1, A_2, A_3, $\hat{A}_1$, $\hat{A}_2$, and $\hat{A}_3$ are equal to those of the original subsystem. The latter are written as

$$A_1 = \begin{vmatrix} 1 & \langle e\rangle \\ \langle e\rangle & \langle e^2\rangle \end{vmatrix}, \quad A_2 = \begin{vmatrix} \langle s\rangle & \langle e\rangle \\ \langle es\rangle & \langle e^2\rangle \end{vmatrix}, \quad A_3 = \begin{vmatrix} \langle s\rangle & 1 \\ \langle es\rangle & \langle e\rangle \end{vmatrix}, \tag{68}$$

$$\hat{A}_1 = \begin{vmatrix} 1 & \langle \hat{e}\rangle \\ \langle \hat{e}\rangle & \langle \hat{e^2}\rangle \end{vmatrix}, \quad \hat{A}_2 = \begin{vmatrix} \langle \hat{s}\rangle & \langle \hat{e}\rangle \\ \langle \hat{es}\rangle & \langle \hat{e^2}\rangle \end{vmatrix}, \quad \hat{A}_3 = \begin{vmatrix} \langle \hat{s}\rangle & 1 \\ \langle \hat{es}\rangle & \langle \hat{e}\rangle \end{vmatrix}. \tag{69}$$

The combination of M pseudosubsystems can then be used as a numerical approximation of the original system for each energy interval [Eq. (49)], i.e.,

$$\text{Original system: } \frac{dP_i}{dt} = \frac{1}{\tau}\left(\langle s\rangle_i - P_i \frac{A_2}{A_1} + \langle e\rangle_i \frac{A_3}{A_1}\right),$$
$$P_i(t=0) = C \sum_j n_j^i e^{-\epsilon_j^i \beta}, \tag{70}$$

$$\text{Pseudosystem: } \frac{d\hat{P}_i}{dt} = \frac{1}{\tau}\left(\langle \hat{s}\rangle_i - \hat{P}_i \frac{\hat{A}_2}{\hat{A}_1} + \langle \hat{e}\rangle_i \frac{\hat{A}_3}{\hat{A}_1}\right),$$
$$\hat{P}_i(t=0) = C N_i e^{-E_i \beta}. \tag{71}$$

Using the time evolution of the pseudosystem, the property evolution of the system, such as that for temperature and entropy, can be determined.

IV. APPLICATION TO AN ISOLATED CHEMICALLY REACTIVE IDEAL GAS MIXTURE

A. System definition and state representation

1. Microstate

The state space of a chemically reactive system is composed of two subspaces, reactant and product. The energy eigenlevels of the reactants and those of the products together form the energy eigenlevels for the system as a whole. Denoting the state space of the reactants by $\mathcal{H}^{\text{reactant}}$ and that of the products by $\mathcal{H}^{\text{product}}$, the system state space $\mathcal{H}$ takes the form

$$\mathcal{H} = \mathcal{H}^{\text{reactant}} \oplus \mathcal{H}^{\text{product}}. \tag{72}$$

The simple yet well-studied chemical reaction mechanism considered here is

$$F + H_2 \Leftrightarrow FH + H \tag{73}$$

since it is well adapted to illustrating our general approach. Reaction mechanisms in the vein of the general Guldberg-Waage chemical relaxation equation are considered in Ref. [32] where the SEAQT framework is used to model coupled reaction mechanisms while in Refs. [33,34] complex, coupled reaction-diffusion pathways are used to predict the effects of microstructural degradation and chromium oxide poisoning on the performance of a solid oxide fuel cell cathode. Predictions made are compared with experimental data. A study of chemical reaction rate is also given in Ref. [18]. In addition, Grmela provides a study using GENERIC [35] of the entropy production that occurs in chemically reactive systems represented by the general Guldberg-Waage chemical relaxation equation.

Now, the available energy eigenvalues for one subspace (reactant or product) are constructed from the energy eigenvalues of each degree of freedom, i.e.,

$$\epsilon^{\text{reactant}} = \epsilon_{t,H_2} + \epsilon_{r,H_2} + \epsilon_{v,H_2} + \epsilon_{t,F}, \tag{74}$$

$$\epsilon^{\text{product}} = \epsilon_{t,FH} + \epsilon_{r,FH} + \epsilon_{v,FH} + \epsilon_{t,H}. \tag{75}$$

The translational energy eigenvalue ϵ_t uses the form of the infinite potential well, the rotational energy eigenvalue ϵ_r the form of the rigid motor, and the vibrational energy eigenvalue ϵ_v the form of the harmonic oscillator, i.e.,

$$\epsilon_t(n_x,n_y,n_z) = \frac{\hbar^2}{8m}\left[\left(\frac{n_x}{L_x}\right)^2 + \left(\frac{n_y}{L_y}\right)^2 + \left(\frac{n_z}{L_z}\right)^2\right], \tag{76}$$

$$\epsilon_r(j,m) = \frac{j(j+1)\hbar^2}{2I} = \frac{j(j+1)\hbar^2}{2\mu r^2}, \tag{77}$$

$$\epsilon_v(\nu) = \left(\nu + \frac{1}{2}\right)\hbar\omega + E_d, \tag{78}$$

where n_x, n_y, and n_z are the quantum numbers for the translational degrees of freedom; j and m are the quantum

numbers for the rotational degrees of freedom; and ν is the quantum number for the vibrational degrees of freedom. ϵ_d is the disassociation energy of a given molecule (e.g., H_2 and FH). Each combination of quantum numbers corresponds to one energy eigenlevel of reactant or product without degeneracy (provided the rotational state is distinguished by the magnetic quantum number m). The system energy eigenlevels are formed by all the available energy eigenlevels of reactants and products. The separation of the two subspaces $\{\epsilon^{\text{reactant}}\}$ and $\{\epsilon^{\text{product}}\}$ is kept to maintain their clear physical meaning. In the modeling, these two subspaces serve as two subsystems in the discussion of system nonequilibrium state.

2. Density of state

For temperatures higher than the characteristic temperatures of translation and rotation, the energy eigenlevels distribute from the ground state to infinity with high density. These spectrums can be approximated to be continuous. The densities of states of translational and rotational energy for species A are given by

$$D_{t,A}(\epsilon)d\epsilon = \frac{2\pi V}{h^3}(2m_A)^{\frac{3}{2}}\epsilon^{\frac{1}{2}}d\epsilon, \tag{79}$$

$$D_{r,A}(\epsilon)d\epsilon = \frac{2I_A}{\hbar^2}d\epsilon. \tag{80}$$

In contrast, that for vibration is assumed to be discrete. To describe the available energy eigenlevels, density of states instead of individual energy eigenlevels are used because of the extremely large number of the latter. Similar to the way of dealing with individual energy eigenlevels, the density of states is calculated separately for reactants and products. The joint density of states from the densities of states of M independent energy forms can be calculated from

$$\begin{aligned} D(E)dE &= \int_{\sum_{i=1}^{M} e_i = E} D_1(e_1)D_2(e_2)\dots D_M(e_M)de_1de_2\dots de_M \\ &= dE\int_{E_1^g}^{E} de_1\int_{E_2^g}^{E-e_1} de_2\dots\int_{E_M^g}^{E-\sum_{i=1}^{M-2}} de_{M-1}D_1(e_1)D_2(e_2)\dots D_{M-1}(e_{M-1})D_M\left(E-\sum_{i=1}^{M-1}e_i\right), \end{aligned} \tag{81}$$

where E_i^g is the ground state for the ith density of states.

Specifically, the density of states for one subsystem of the system studied can be calculated by

$$D_{\text{reac}}(E)dE = \int_{\epsilon_{t,H_2}+\epsilon_{r,H_2}+\epsilon_{v,H_2}+\epsilon_{t,F}=E} D_{t,H_2}(\epsilon_{t,H_2})D_{r,H_2}(\epsilon_{r,H_2})D_{v,H_2}(\epsilon_{v,H_2})D_{t,F}(\epsilon_{t,F})d\epsilon_{t,H_2}d\epsilon_{r,H_2}d\epsilon_{v,H_2}d\epsilon_{t,F}, \tag{82}$$

$$D_{\text{prod}}(E)dE = \int_{\epsilon_{t,FH}+\epsilon_{r,FH}+\epsilon_{v,FH}+\epsilon_{t,H}=E} D_{t,FH}(\epsilon_{t,FH})D_{r,FH}(\epsilon_{r,FH})D_{v,FH}(\epsilon_{v,FH})D_{t,H}(\epsilon_{t,H})d\epsilon_{t,FH}d\epsilon_{r,FH}d\epsilon_{v,FH}d\epsilon_{t,H}. \tag{83}$$

The joint distribution of the density of states of translational and rotational energy eigenlevels takes the form

$$\begin{aligned} D_{t,r}^{\text{reac}}(E)dE &= \int_{\epsilon_{t,H_2}+\epsilon_{r,H_2}+\epsilon_{t,F}=E} D_{t,H_2}(\epsilon_{t,H_2})D_{r,H_2}(\epsilon_{r,H_2})D_{t,F}(\epsilon_{t,F})d\epsilon_{t,H_2}d\epsilon_{r,H_2}d\epsilon_{t,F} \\ &= \frac{2\pi V}{h^3}\left(2m_{H_2}\right)^{\frac{3}{2}}\frac{2\pi V}{h^3}(2m_F)^{\frac{3}{2}}\frac{2I_{H_2}}{\hbar^2}\frac{1}{3}B\left(\frac{3}{2},\frac{3}{2}\right)d\epsilon, \end{aligned} \tag{84}$$

$$\begin{aligned} D_{t,r}^{\text{prod}}(E)dE &= \int_{\epsilon_{t,FH}+\epsilon_{r,FH}+\epsilon_{t,H}=E} D_{t,FH}(\epsilon_{t,FH})D_{r,FH}(\epsilon_{r,FH})D_{t,H}(\epsilon_{t,H})d\epsilon_{t,FH}d\epsilon_{r,FH}d\epsilon_{t,H} \\ &= \frac{2\pi V}{h^3}(2m_{FH})^{\frac{3}{2}}\frac{2\pi V}{h^3}(2m_H)^{\frac{3}{2}}\frac{2I_{FH}}{\hbar^2}\frac{1}{3}B\left(\frac{3}{2},\frac{3}{2}\right)d\epsilon, \end{aligned} \tag{85}$$

where $B(\dots,\dots)$ is the beta function. Generally, the energy eigenlevels for a subspace are constructed from t translational and r rotational degrees of freedom, and the density of states for the subsystem built from these eigenlevels takes the form

$$D_{t,r}(E)dE \propto E^{\frac{1}{2}t+r-1}dE. \tag{86}$$

For temperatures not much greater than or less than or equal to the characteristic temperature of the vibrational degrees of freedom, the form of the density of state for each subsystem is, respectively,

$$D^{\text{reac}}(E-\epsilon_{d,H_2})dE = D_{t,r}^{\text{reac}}(E)dE, \tag{87}$$

$$D^{\text{prod}}(E-\epsilon_{d,FH})dE = D_{t,r}^{\text{reac}}(E)dE, \tag{88}$$

where ϵ_{d,H_2} and $\epsilon_{d,FH}$ are the ground energy of vibrational degrees of freedom of H_2 and FH, which are approximated by the disassociation energies of H_2 and FH.

For temperatures much greater than the characteristic temperature of the vibrational degrees of freedom, the form of the density of state for each subsystem is, respectively,

$$D^{\text{reac}}(E)dE = dE\sum_{\nu,\epsilon_{v,H_2}<E} D_{t,r}^{\text{reac}}(E-\epsilon_{v,H_2}), \tag{89}$$

$$D^{\text{prod}}(E)dE = dE\sum_{\nu,\epsilon_{v,FH}<E} D_{t,r}^{\text{prod}}(E-\epsilon_{v,FH}). \tag{90}$$

Finally, the energy eigenlevel information for reactant ($\{\epsilon_i^{\text{reactant}}\}$ and $\{n_i^{\text{reactant}}\}$) and product ($\{\epsilon_j^{\text{product}}\}$ and $\{n_j^{\text{product}}\}$) is

obtained. The system has energy eigenlevels $\{\epsilon_i^{\text{reactant}},\epsilon_j^{\text{product}}\}$ and density of states $\{n_i^{\text{reactant}},n_j^{\text{product}}\}$.

B. Numerical process

1. Cutoff energy

With the density of states for each subspace, the cutoff energy for the system at a fixed energy corresponding to an initial state or that of stable equilibrium can easily be calculated. Given the density of states $n(E)$ of a subsystem and a type of probability distribution with parameter θ which takes the form that reduces to the canonical distribution when $\theta = 0$, i.e.,

$$p(E) \propto D(E)E^{\theta}e^{-\beta E}, \tag{91}$$

the cumulative distribution function becomes

$$F(E) \propto \int_{E_{\text{ground}}}^{E} D(E')E^{\theta}e^{-\beta E'}dE'. \tag{92}$$

The cutoff energy is then the inverse of the cumulative distribution function F where δ is a very small number, namely,

$$E_{\text{cut}} = F^{-1}(1-\delta). \tag{93}$$

As an example, take a system consisting of an ideal gas mixture that has a temperature lower than the characteristic temperature of vibration but higher than that of translation and rotation. This is indicative of the conditions for a very large number of ideal gas applications (10^2 K $\sim 10^3$ K). The energy eigenlevels for a subspace are constructed from t translational and r rotational degrees of freedom, and the density of states for the subsystem built from these eigenlevels takes the form

$$D_{t,r}(E) = C_0E^{\frac{1}{2}t+r-1}, \tag{94}$$

where the procedure for determining C_0 is given in previous section [e.g., see Eqs. (84) and (85)]. If the probability distribution in the subsystem is a gamma function with parameters β and θ, then

$$p(E) \propto D_{t,r}(E)E^{\theta}e^{-\beta E} \propto E^{\alpha+\theta-1}e^{-\beta E} \propto \Gamma(\alpha+\theta,\beta). \tag{95}$$

The distribution among the subsystem energy eigenlevels yields to the gamma distribution $\Gamma(\alpha+\theta,\beta)$ with the following parameter definitions:

$$\alpha = \frac{1}{2}t + r, \quad \beta = \frac{1}{k_bT}. \tag{96}$$

The distribution and cumulative distribution functions then take the form

$$p(E) = \frac{E^{\alpha+\theta-1}e^{-\beta E}}{\int_0^{\infty} E'^{\alpha+\theta-1}e^{-\beta E'}dE'} = \frac{\beta^{\alpha+\theta}}{\Gamma(\alpha+\theta)}E^{\alpha+\theta-1}e^{-\beta E}, \tag{97}$$

$$F(E) = \frac{\int_{\approx 0}^{E} E'^{\alpha+\theta-1}e^{-\beta E'}dE'}{\int_0^{\infty} E'^{\alpha+\theta-1}e^{-\beta E'}dE'} = \frac{\gamma(\alpha+\theta,\beta E)}{\Gamma(\alpha+\theta)}, \tag{98}$$

where $\Gamma(\alpha+\theta)$ is the gamma function evaluated at $\alpha+\theta$, and $\gamma(\alpha+\theta,\beta E)$ is the lower incomplete gamma function. The energy of the ground state is approximately zero. The cutoff energy is found from the inverse of the cumulative distribution function such that

$$E_{\text{cut}} = F^{-1}(1-\delta;\alpha+\theta,\beta). \tag{99}$$

2. Pseudosystem

Since there are two subspaces for the chemically reactive system considered here, i.e., one for reactants and the other for products, two cutoff energies are calculated; and the larger one is used to truncate the open interval of infinite energy eigenlevels into a closed one. To establish the pseudosystem, an energy interval ΔE is chosen according to the quasicontinuous condition (55). Two pseudosubsystems are then set up, one for the reactants and the other for the products. The pseudosystem for the composite system is the combination of the two pseudosubsystems. The energy eigenvalue and degeneracy for one pseudosubsystem corresponding to the ith interval are then determined by integrating Eqs. (50) and (51) over that interval where the summations are replaced by integrals using the density of states $D(E)$ so that

$$N_i = \int_{e_i}^{e_i+\Delta E} D(E)dE, \tag{100}$$

$$E_i = \frac{1}{N_i}\int_{e_i}^{e_i+\Delta E} D(E)E\,dE. \tag{101}$$

Using Eq. (86) and considering only translational and rotational degrees of freedom, the energy eigenvalue and degeneracy for the ith energy interval is

$$N_i = C_0\int_{e_i}^{e_i+\Delta E} E^{\alpha-1}dE = \frac{C_0}{\alpha}\left[(e_i+\Delta E)^{\alpha} - e_i^{\alpha}\right], \tag{102}$$

$$E_i = \frac{C_0}{N_i}\int_{e_i}^{e_i+\Delta E} E^{\alpha}dE = \frac{\alpha}{\alpha+1}\frac{(e_i+\Delta E)^{\alpha+1} - e_i^{\alpha+1}}{(e_i+\Delta E)^{\alpha} - e_i^{\alpha}}, \tag{103}$$

where C_0 and α are defined by Eqs. (94) and (96), respectively, and calculated via Eqs. (82) and (83). Once the pseudosystem has been defined in this way, the evolution of the isolated chemically reactive system can be determined.

C. Initial condition

We provide the analytical solution for an initial condition when the vibrational energy is frozen.

1. Initial condition 1: Second-order hypoequilibrium

For a second-order hypoequilibrium state, it is assumed that the reactant energy eigenlevels and product energy eigenlevels form subspaces, respectively. In either subspace, the distribution is proportional to the canonical distribution. Using Eqs. (84), (85), (87), and (88),

$$p^{\text{reac}}(E-\epsilon_{d,H_2})dE = p_{t,r}^{\text{reac}}(E)dE \propto D_{t,r}^{\text{reac}}(E)e^{-\beta E}dE \propto E^3e^{-\beta E}dE, \tag{104}$$

$$p^{\text{prod}}(E-\epsilon_{d,FH})dE = p_{t,r}^{\text{prod}}(E)dE \propto D_{t,r}^{\text{prod}}(E)e^{-\beta E}dE \propto E^3e^{-\beta E}dE. \tag{105}$$

Both distributions are $\Gamma(4,\beta)$ gamma distributions and both normalization constants are $\beta^4/\Gamma(4)$, where $\Gamma(4)$ is calculated from the gamma function.

2. *Initial condition 2: The gamma distribution*

If the initial condition for one subspace (reactant or product) takes the general form of a gamma distribution, then, for example, the reactant subspace distribution is given by

$$p^{\text{reac}}(E-\epsilon_{d,H_2})dE \propto E^{3+\theta}e^{-\beta E}dE \tag{106}$$

since the product has little probability initially. Equation (106) is the gamma distribution $\Gamma(4+\theta,1/\beta)$. The mean and variance of E take the form

$$\text{Mean} = \frac{4+\theta}{\beta}, \tag{107}$$

$$\text{Var} = \frac{4+\theta}{\beta^2}. \tag{108}$$

By varying θ, the influence of the initial condition can be studied. For instance, the effusion process can result in a gamma distribution if the probability distribution of one of the reactant's (e.g., F) energy eigenlevels is

$$p^F(E)dE = p_t^F(E)dE = \beta^2 E e^{-\beta E}dE. \tag{109}$$

This is the energy distribution of an effusion particle, which can be acquired from the velocity distribution

$$F(v)dv \propto v f_M(v)dv \propto v \times v^2 e^{-\frac{mv^2}{2k_bT}}dv, \tag{110}$$

where f_M is the Maxwellian velocity distribution. The other reactant H_2 has the Maxwellian probability distribution of its energy eigenlevels given by

$$p_{t,r}^{H_2}(E)dE = \frac{D_{t,r}^{H_2}(E)e^{-\beta E}}{Z_{t,r}^{H_2}(\beta)}dE = \frac{\beta^{5/2}}{\Gamma(5/2)}E^{3/2}e^{-\beta E}dE, \tag{111}$$

where $D_{t,r}^{H_2}$ is the density of state for H_2 with vibrational degrees of freedom frozen, and $Z_{t,r}^{H_2}$ is the partition function. This results in a gamma distribution for $\theta = 0.5$ in Eq. (106). The initial reactant state is then

$$\begin{aligned} &p^{\text{reac}}(E-\epsilon_{d,H_2})dE \\ &= p_{t,r}^{\text{reac}}(E) = \int_0^E p^F(E-e_1)p^{H_2}(e_1)de_1 \\ &= \frac{\beta^{9/2}}{\Gamma(9/2)}E^{7/2}e^{-\beta E}dE. \end{aligned} \tag{112}$$

V. RESULTS AND DISCUSSION

A. Second-order hypoequilibrium initial condition

The fundamental theoretical result for the SEA equation of motion is composed of two parts: the nonequilibrium kinetic trajectory in state space and the subsystem temperatures. SEA predicts a unique trajectory for nonequilibrium state evolution (Sec. II E), while the definition of subsystem and subsystem temperature (Sec. II F) provides a good framework for studying the trajectory. Unlike phenomenological definitions of nonequilibrium temperature, the subsystem temperature defined here is fundamental and has a clear physical picture: the temperature is defined via the canonical distribution. Furthermore, the principle of SEA leads to a set of very well-defined physical and mathematical features for subsystem temperature, which allow subsystem hypoequilibrium state and temperature to be reasonable generalizations of the existing concepts of state and temperature at stable equilibrium. In order to illustrate the above ideas, the nonequilibrium behavior of the isolated chemically reactive system introduced earlier is modeled using the SEAQT framework. A discussion of results for the state evolution trajectory in state space and on an energy-entropy (E-S) diagram is given first followed by a discussion of results for the total probability and temperature of the subsystems.

The initial state of the system is chosen to be a second-order hypoequilibrium state, and the two subsystems are the reactant and product subspaces. The temperatures of the two subsystems for the initial nonequilibrium state are selected to be 300 K and 400 K, respectively. Although it would be more reasonable to choose the same temperature, the temperatures chosen here are to better illustrate subsystem temperature evolution. The total probability in the reactant subsystem is 0.9999, and that in the product subsystem 0.0001. The cutoff energy is 5.76×10^{-19} J, and the energy interval is 8.84×10^{-23} J. As a comparison, the real energy eigenlevel interval is 2.62×10^{-43} J, and the interval calculated with the initial temperature is $1/\beta(t=0) = 6.9 \times 10^{-21}$ J. Thus, the quasicontinuous condition holds. There are 14 127 energy eigenlevels in the reactant subspace (or subsystem) and 16 666 energy eigenlevels in the product subspace (or subsystem). At the initial state, the system has more than a 0.999 999 probability of being distributed in the 3500 energy eigenlevels below the cutoff energy of 5.76×10^{-19} J. Thus, a total of 30 793 levels are used to represent with great accuracy (as demonstrated below) the estimated 10^{130} levels of the actual system. The relaxation time is chosen to be 1 so that the kinetics of state evolution is studied using dimensionless time.

Figure 1(a) shows the system state evolution trajectory on an energy-entropy diagram [36]. For any state of the system (nonequilibrium or equilibrium), the system state can be mapped to one point on the energy-entropy diagram. The bold solid concave curve is the stable equilibrium curve, and any point on the curve represents a stable equilibrium state. Because the stable equilibrium state has the maximum entropy at a given energy, composition, and volume, there is no system state available to the right of the stable equilibrium curve. Point A_0 is the initial state in the chemically reactive model. If the system state evolution trajectory is mapped from state space to the energy-entropy diagram, the trajectory is a horizontal line (red line) at a given energy. Points A_1 to A_4 are four intermediate nonequilibrium states on the evolution trajectory, and point B on the concave curve is the stable equilibrium state.

Figure 1(b) shows the changes in the entropy and entropy generation rate values as the system state evolves along the trajectory. The entropy generation rate is not constant along the dimensionless time axis. According to SEA, the entropy generation rate is proportional to $\boldsymbol{g}_{S\perp L(\boldsymbol{g}_I,\boldsymbol{g}_E)}$, which lies parallel to the constant probability and constant energy hypersurface and is the perpendicular component of the

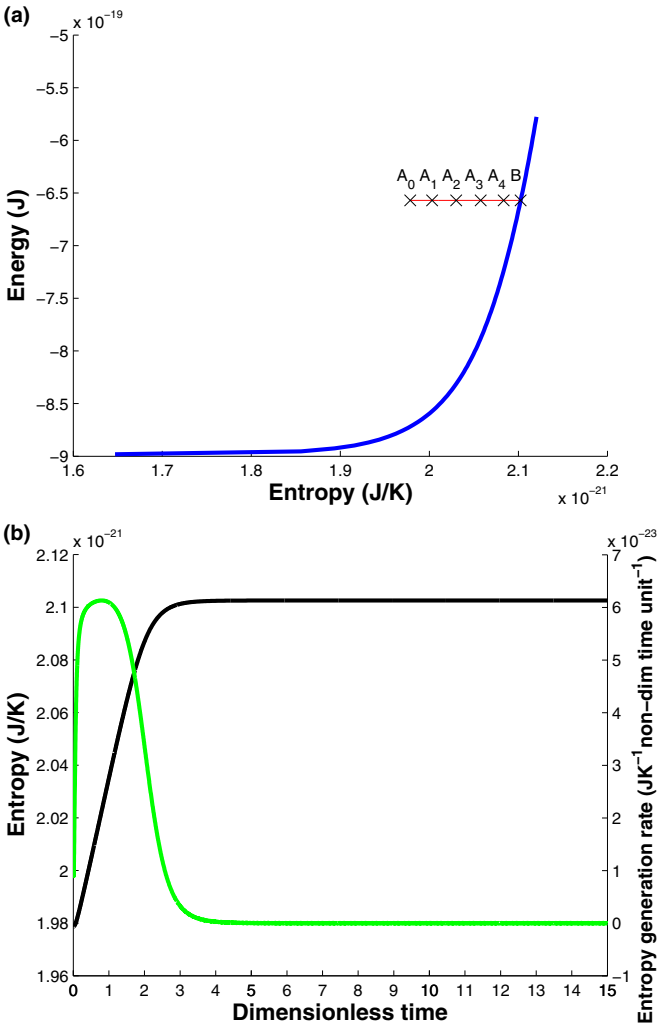

FIG. 1. (a) System state evolution trajectory on an energy-entropy diagram; (b) entropy (black line) and entropy generation rate [green (light gray) line] evolutions as a function of dimensionless time.

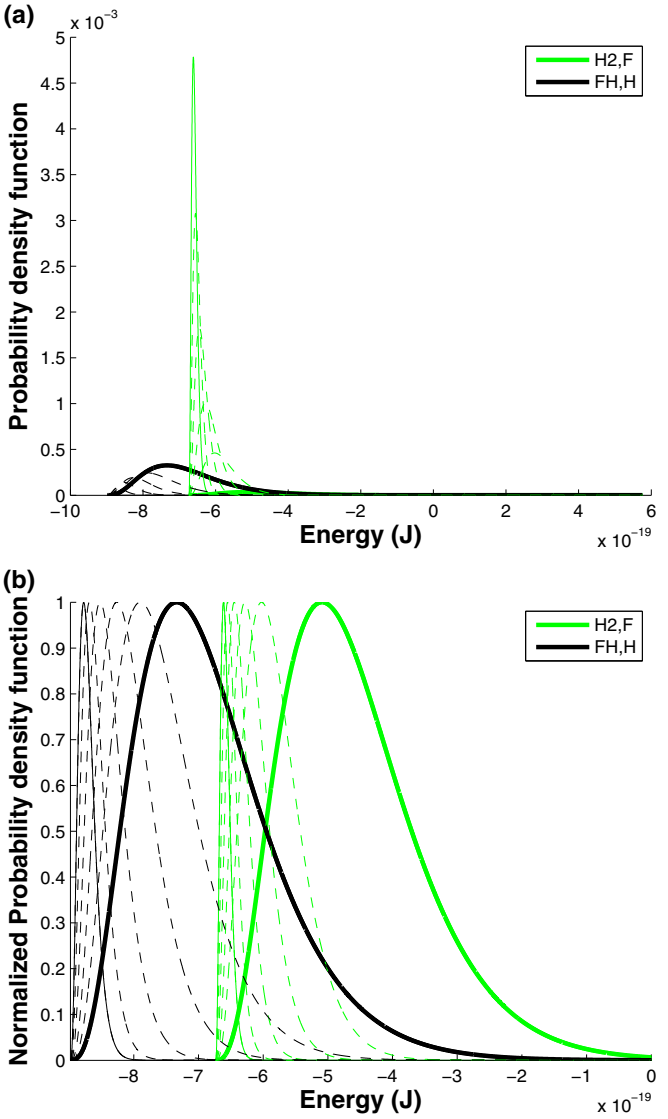

FIG. 2. System trajectory in state space represented by (a) the evolution of the probability distribution among the energy eigenlevels and by (b) the evolution of the normalized distributions. The four dashed lines correspond to four of the nonequilibrium states along the trajectory (states A_1 to A_4 in Fig. 1), while the single narrow solid line is the distribution for the initial state (A_0) and the single bold solid line is that for the equilibrium state (B).

entropy gradient to the manifold $L(\boldsymbol{g}_I, \boldsymbol{g}_E)$. Thus, the entropy generation rate reveals the entropy gradient changes along the trajectory in state space.

Figure 2(a) shows the probability distribution among the energy eigenlevels when the system is at states A_0 to A_4 and B in Fig. 1(a). In order to better show each distribution's evolution, each curve is normalized by its peak and the result shown in Fig. 2(b). In Fig. 2(a), one can observe that the system probability transfers from the reactant subsystem to the product subsystem. At the same time, the distributions of both subsystems evolve from narrow to wider distributions, indicating that the temperature is increasing. The distributions remain canonical at all times. The distribution evolution for each subsystem is more clearly seen in Fig. 2(b).

As discussed in Sec. II F, the nonequilibrium evolution of state can be described via the evolutions of $\alpha_p(t)Z_p[\beta_p(t)]$ and $\beta_p(t)$, which correspond to the particle number $N_p(t)$ and temperature $T_p(t) = 1/k_b\beta_p(t)$. Z_p is the partition function of the subsystem. Given the evolution of the particle number and temperature, one can rebuild the probability distribution via Eq. (38). Figure 3(a) shows the particle number evolution for the process in which reactant changes to product. Figure 3(b) shows the temperature evolution. The energy released by the chemical reaction heats up both the reactant and product, and the manner in which the temperature increases follows the SEA trajectory. At the end, when the system reaches stable equilibrium, the temperatures of the subsystems are equal, and the nonequilibrium temperatures converge to that for stable equilibrium. As already indicated in the discussion above surrounding Fig. 2(b), the physical meaning of this temperature increase is a broadening in the probability distribution among the energy eigenlevels.

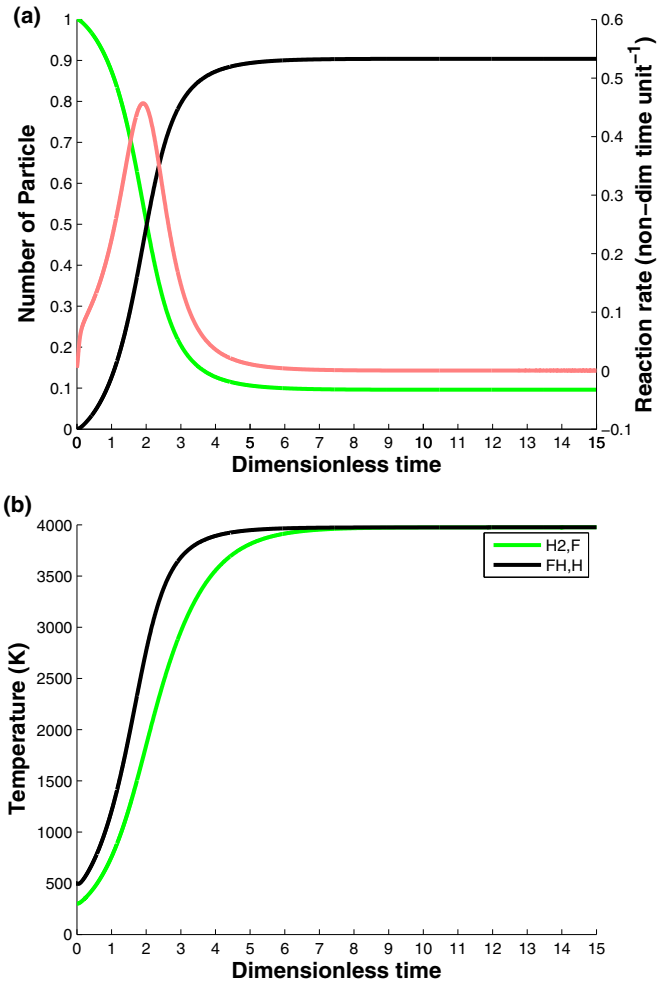

FIG. 3. (a) Evolutions of particle number and reaction rate and (b) the evolution of temperature. For the line colors in (a), the black line and the green (light gray) line represent the FH, H and H_2, F, respectively, and the red (dark gray) line represents reaction rate.

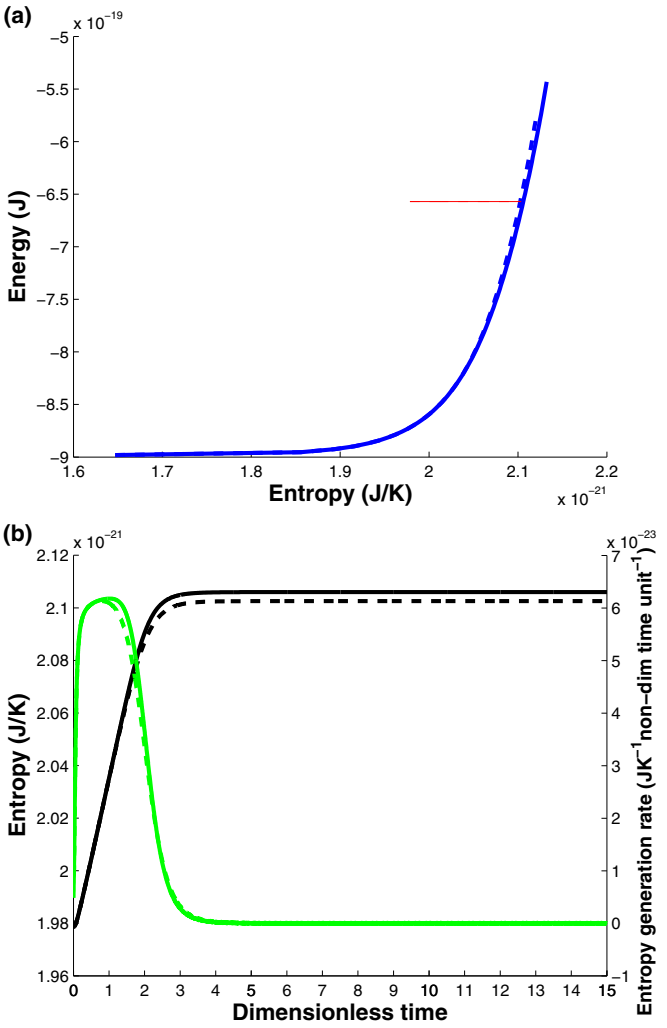

FIG. 4. Comparison of (a) the energy-entropy diagrams and (b) the entropy (black line) and entropy generation rate [green (light gray) line] evolutions for a system with and without vibrational degrees of freedom. The solid lines are for the system with vibrational energy eigenlevels, while the dashed lines are for the system without vibrational levels.

B. Influence of the density of states

Using a comparison of system state evolution with and without vibrational energy eigenlevels included in the system description, one can study how the density of states influences system behavior. Figure 4(a) shows the comparison of the corresponding stable equilibrium curves and the evolution trajectory using the same initial subsystem temperatures. Because the stable equilibrium temperature is less than 4000 K [Fig. 3(b)] and the characteristic temperature of vibration is about 6000 K, the stable equilibrium curves show some difference, which is consistent with the result found from equilibrium thermodynamics. Figure 4(b), in contrast, shows the difference of the two systems in the nonequilibrium region. At the beginning, the two systems perform the same. As the entropy generation rate approaches the maximum, the two systems perform differently and the system with vibrational energy eigenlevels exhibits a larger entropy and entropy generation rate. This phenomenon can be explained using subsystem temperature. The initial temperature is about one order of magnitude less than the characteristic temperature of vibration, which leads to the vibrational energy eigenlevels being frozen. Thus, the two systems perform similarly. However, as each subsystem temperature increases [Fig. 3(b)], the vibrational energy eigenlevels are activated, resulting in a difference in performance between the two systems.

Figure 5(a) shows the difference in the system stable equilibrium distributions with and without vibrational energies. Figure 5(b) shows the density of states difference. One can observe that although total properties such as the entropy change little, the probability distribution and even the equilibrium particle number changes are somewhat more significant. All the differences result from the density of states changing.

C. Influence of the initial condition on the trajectory

Another important study is for the case when the initial condition is a very high order hypoequilibrium state. In that

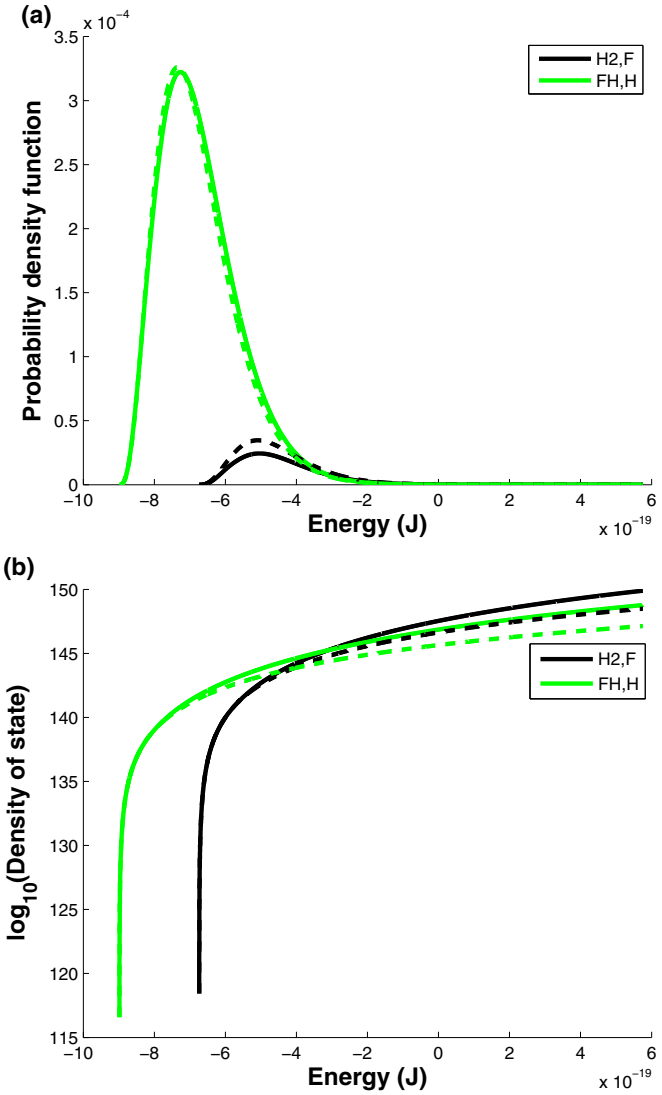

FIG. 5. Comparison of (a) the stable equilibrium distributions and (b) the density of states for the systems with (solid line) and without (dashed line) vibrational energy eigenlevels.

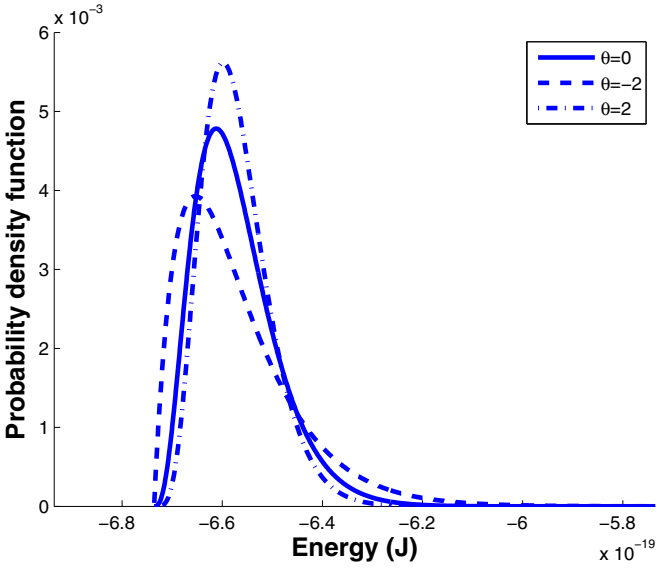

FIG. 6. Initial distribution in reactant subspace for $\theta = 0$ (solid line), $\theta = -2$ (dashed line), and $\theta = 2$ (dashed-dotted line).

case, although the theoretical discussion in Sec. II F is still valid, the number of subsystem divisions of the system may be so high that characterizing each nonequilibrium state as an Mth-order hypoequilibrium state may no longer be practical. However, the density of states method still permits the solution of the equation of motion to very high accuracy. This section uses the general gamma distribution to study the influence of initial condition on the nonequilibrium trajectory by varying θ in Eq. (106). The mean value of the energy for three cases with different θ's is chosen to be the same in order to ensure the same system total energy and the same final stable equilibrium state. From Eqs. (111) and (112), the ratio of β in the three cases is $\beta_{-2} : \beta_0 : \beta_2 = 1 : 2 : 3$ and the ratio of the variance of energy is $\mathrm{Var}_{-2} : \mathrm{Var}_0 : \mathrm{Var}_2 = 1 : 1/2 : 1/3$. The initial distribution for the reactant subspace is shown in Fig. 6, which takes 0.9999 of the total probability. It can be observed that for lower θ, there is more probability distributed in the higher energy eigenlevels (energies greater than -6.4×10^{-19} J) and the energy variance is larger.

The evolution in dimensionless time is studied in Fig 7. In order to facilitate the comparison, all the curves are shifted such that time 0 is the dimensionless time when the maximum reaction rate is reached, and both Figs. 7(a) and 7(b) use the same 0 time. In Fig. 7(a), it is observed that the beginning of the three cases is quite different, while the reaction processes after time 0 are similar. Furthermore, the negative θ case takes less time to arrive at stable equilibrium than the zero θ case (Maxwellian distribution), and the positive θ case takes even more. In Fig. 7(b), the entropy evolution is also similar after time 0. However, the beginning parts of the evolution exhibit three features. The first is that the initial entropy of the negative and positive θ cases are both smaller than that for $\theta = 0$ since the Maxwellian distribution provides the largest entropy for given energy. That also means that the initial entropy cannot decide how fast the reaction process is, which instead is decided by the value and the sign of θ. The second feature is that for negative θ, the entropy evolution is faster than that for the zero θ case, and the maximum of the entropy generation rate is larger than that for the zero θ case. The opposite is the case for the positive θ case. Both Figs. 7(a) and 7(b) show that the negative θ provides the faster reaction process. One possible explanation is that for lower θ, more probability is distributed in the higher energy eigenlevels, which accelerates the reaction process. Another view is that the lower θ case has lower β, which phenomenologically can be explained as higher temperature. The final or third feature is that in the evolution after time 0, the probability distributions for the positive and negative cases are not Maxwellian distributions in the strict sense used in the next section even though the particle number and entropy evolution are almost the same. However, as shown in Figs. 7 and 8, a Maxwellian distribution in each subspace, for a second-order hypoequilibrium state, can be a very good approximation for studying a reaction's intermediate nonequilibrium states.

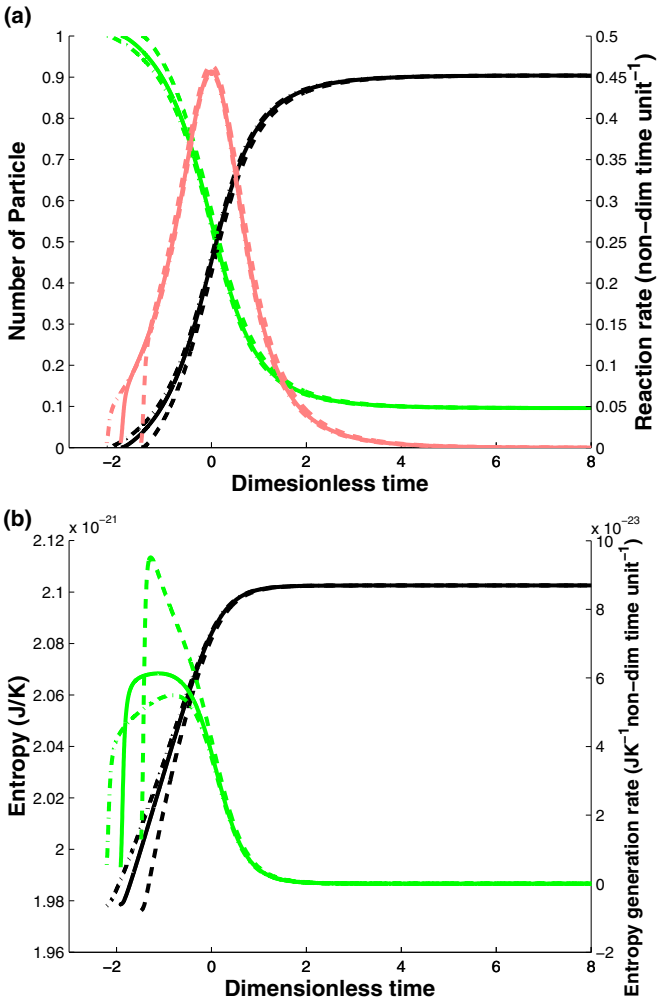

FIG. 7. (a) Evolutions of particle number and reaction rate. For the line colors in (a), the black line and green (light gray) line represent the FH, H and H_2, F, respectively, and the red (dark gray) line represents reaction rate. (b) Evolutions of entropy (black line) and entropy generation rate [green (light gray) line]. For the line styles in both figures, $\theta = 0$ (solid line), $\theta = -2$ (dashed line), and $\theta = 2$ (dashed-dotted line). The dimensionless time when the maximum reaction rate is reached is set to be 0.

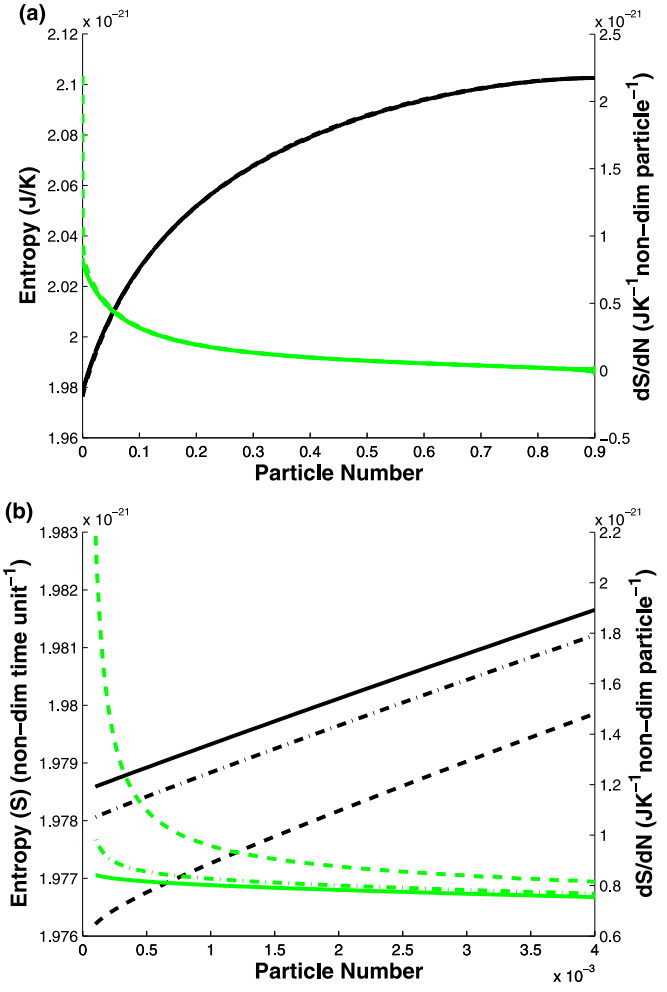

FIG. 8. Trajectory representation using product particle number and entropy. Range of product particle number (a) from 0 to 0.9 and (b) from 0 to 0.004. The black line and the green (light gray) line represent entropy (S) and dS/dN, respectively. For the line styles, $\theta = 0$ (solid line), $\theta = -2$ (dashed line), and $\theta = 2$ (dashed-dotted line).

In Fig. 8, the trajectory of the chemical reaction is illustrated using the product particle number and system entropy. The particle number of the product can be regarded as an equivalent variable to the reaction coordinate here. By using product particle number instead of dimensionless time, only the information of the intermediate states is kept. It must be pointed out here that in Fig. 8, any trajectory with a positive dS/dN, i.e., a monotonically increasing function linking the initial state and stable equilibrium, does not violate the second law of thermodynamics. However, the trajectories plotted are not just any trajectories but those uniquely predicted by SEA, the maximum-entropy-production (MEP) trajectories. It can be observed that the trajectories for the three θ's chosen are very similar in Fig. 8(a) except at the very beginning [shown in Fig. 8(b)]. As mentioned before, even though the probability distributions do not become second-order hypoequilibrium distributions until very late (after the product particle number reaches 0.5), the second-order hypoequilibrium state can provide a very good approximation of the intermediate nonequilibrium states. In addition, in Fig. 8(b), one can observe that the zero θ case has the largest initial entropy and lowest dS/dN. The trajectories at the beginning can be separated into two parts by the state which the particle number reaches at 0.002. From 0 to 0.002, dS/dN for the nonzero θ case has a huge difference with that for the zero θ case. If the entropy is used as the measure of the difference of the distributions, the larger difference results in a greater speed of the non-Maxwellian distribution approaching the Maxwellian one. In this process, the degree of reaction only changes a little when compared with the change in the total particle number of the product. After the particle number reaches 0.002, there is little difference in dS/dN between the three cases, even though the difference in entropy lasts until the system distribution reaches that for a second-order hypoequilibrium state. However, this difference is small when compared with the total system entropy. Recall from Fig. 7

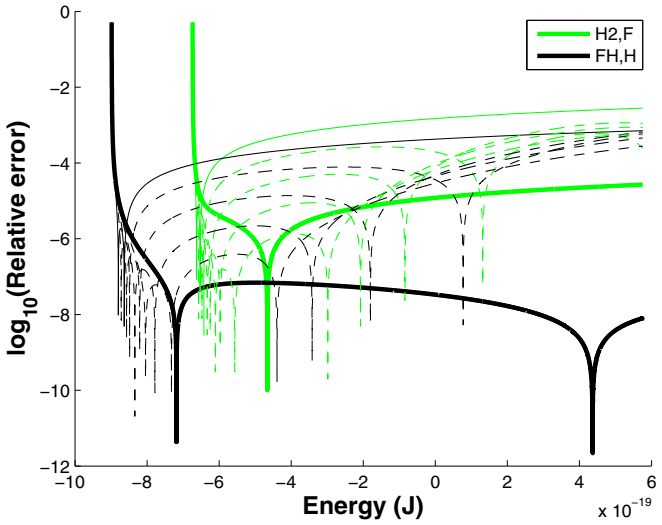

FIG. 9. Relative error for the probability distribution.

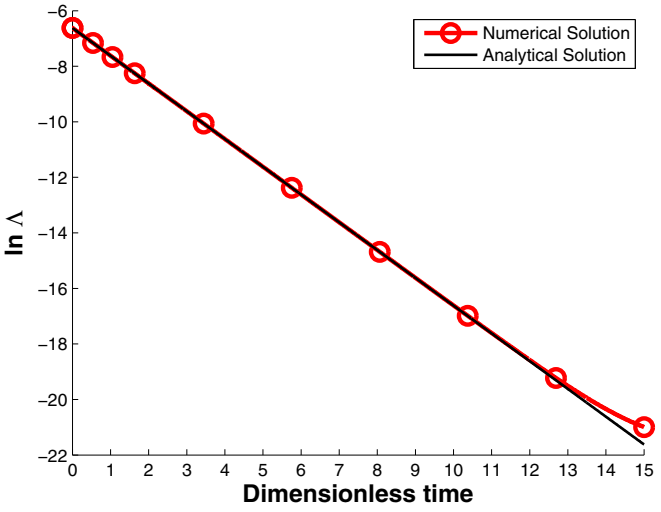

FIG. 10. Time evolution of Λ.

that there is quite a big difference in the state evolutions for the three cases until time 0, when the product particle number reaches about 0.5. For the range of product particle number from 0.002 to 0.5, the difference in entropy is negligible for the intermediate states of the trajectory but nonetheless has a large influence on the evolution in dimensionless time.

D. Numerical error

In Fig. 9, the state of the system without vibrational energy eigenlevels is compared with the analytical solution of the state, the gamma function, since the analytical solution for a system with vibrational levels is difficult to acquire. Figure 9 shows the relative difference of the numerical solution with the analytical solution at states A_0 to A_4 and B. The relative errors of almost all the energy eigenlevels are less than 10^{-2}. There are 14 out of the 30 793 eigenlevels where the relative error is larger than 10^{-2}. However, the total probability for these levels is less than 6.5×10^{-8}. The error is larger for these energy eigenlevels since they coincide with the region where the density of states is lower and increasingly steep. Thus, this error can be explained by truncation error. It is also observed that the error is larger at the initial state than that at stable equilibrium. In addition, the states at lower subsystem temperatures have narrower distributions, whose accuracy is limited by the quasicontinuous condition. The energy interval chosen is about 10^{-2} times lower than $1/\beta = k_b T$, and that accuracy sets an upper limit on the relative error at the initial state. In conclusion, the density of states method developed and used here provides a very accurate numerical solution to the SEAQT equation of motion for a system with a very large number of energy eigenlevels. Furthermore, the criterion used in the previous section to check whether a distribution is Maxwellian or not is determined from the study here, i.e., if a distribution of energy has its distribution across most of the energy eigenlevels (for example, 99% of them) very close to the Maxwellian distribution (relative difference less than 1%) with the same mean value of energy, the distribution is regarded as a Maxwellian distribution.

Finally, validation of the numerical accuracy of the time evolution can be acquired through a value defined by

$$\Lambda = k_b(\beta^{\text{product}} - \beta^{\text{reactant}}) = 1/T^{\text{product}} - 1/T^{\text{reactant}}. \tag{113}$$

According to Sec. II F, β^{product} and β^{product} yield to ODE (42) with different initial temperatures. Subtracting the ODE equations for β^{product} and β^{product} results in

$$\frac{d\Lambda}{dt} = -\frac{1}{\tau}\Lambda, \quad \Lambda(0) = 1/300 - 1/500. \tag{114}$$

Using the dimensionless time scale for $\tau = 1$, the analytical solution of $\ln \Lambda$ yields

$$\ln \Lambda(t) = \ln(1/300 - 1/500) - t = -6.6201 - t. \tag{115}$$

Plotting $\ln \Lambda$ as a function of dimensionless time as is done in Fig. 10 shows the accuracy of the numerical solution for different times. The deviation starts from time 12 onward. At dimensionless time 12, Λ, which is the difference in the inverse of the reactant and product temperatures, has a value smaller than 10^{-8}. Thus, this validation proves that the density of states method can provide an accurate numerical solution for the equation of motion.

VI. CONCLUSIONS

In the preceding study, the nonequilibrium state evolution trajectory for a chemical reaction process is predicted using a first-principles, thermodynamic-ensemble based approach, which provides a computationally simpler, alternative global method for predicting the chemical kinetics of systems. This is well illustrated via the definition of hypoequilibrium state and the existence of canonical distributions outside the realm of stable equilibrium. The nature of the SEA equation of motion directly leads to the existence of a unique nonequilibrium evolution trajectory in state space, which represents the kinetics. With the categorization of nonequilibrium states by different ordered hypoequilibrium states, subsystem and

subsystem temperatures serve as a good description of the trajectory in high-dimensional state space, whose properties are ensured by the equation of motion or the principle of SEA. In addition, with the goal of being able to model systems with a very large number of energy eigenlevels (for the system considered here, on the order of 10^{130}), the concepts of degeneracy and density of states are utilized, and the equation of motion for the degenerate system is developed. The equation of motion for an energy interval is presented and the numerical process to solve it introduced.

The clear physical meaning of the evolution trajectory, subsystem, and subsystem temperature are shown in the results as are the chemical reaction process via particle number evolution and subsystem heating via temperature evolutions. This work provides a reasonable generalization of the concept of temperature at stable equilibrium and offers a framework to describe and study nonequilibrium states and their relaxation process. In addition, even if the order of the hypoequilibrium state is very high so that using this concept in such a case may not be practical, the density of state method still permits solution of the equation of motion so that the nonequilibrium thermodynamic trajectory, especially that for the intermediate states of the system, can be determined with the SEAQT equation of motion. As to the influence of the initial state, it is shown that a second-order hypoequilibrium state is a good approximation for determining the nonequilibrium thermodynamic trajectory when the initial condition or state is that of a gamma distribution for the two subsystems. It is worth noting that although the results given in this paper are based on a two-subsystem division and second-order hypoequilibrium state, the approach presented here can be easily applied to a system with a much higher number of subsystems. What order of hypoequilibrium state is sufficient for arriving at an approximation is left as an open question for future work.

Finally, different from other methods for studying nonequilibrium systems, which are phenomenological or based on mechanics, this paper introduces a practical alternative approach based on a first-principles thermodynamic framework for studying the relaxation of nonequilibrium states.

ACKNOWLEDGMENT

Funding for this research was provided by the US Office of Naval Research under Award No. N00014-11-1-0266.

APPENDIX A: PSEUDOSYSTEM

In this Appendix, a system property calculated by the density of states method developed here is proven to be a good approximation of the property's true value. For the moment of energy in each interval of a given subspace (subsystem),

$$\sum_j n_j^i \left(\epsilon_j^i\right)^\theta = E_i^\theta \sum_j n_j^i \frac{\left(\epsilon_j^i\right)^\theta}{E_i^\theta} = E_i^\theta \sum_j n_j^i \left(1 - \frac{\epsilon_j^i - E_i}{E_i}\right)^\theta$$
$$= E_i^\theta \sum_j n_j^i \left(1 - \theta \frac{\epsilon_j^i - E_i}{E_i}\right) = N_i E_i^\theta, \qquad \text{(A1)}$$

$$\sum_j n_j^i \left(\epsilon_j^i\right)^\theta \ln\left(\epsilon_j^i\right) = \ln(E_i) \sum_j n_j^i \left(\epsilon_j^i\right)^\theta + n_j^i \left(\epsilon_j^i\right)^\theta \ln\left(\frac{\epsilon_j^i}{E_i}\right)$$
$$= \ln(E_i) \sum_j n_j^i \left(\epsilon_j^i\right)^\theta \left(-\frac{\epsilon_j^i - E_i}{E_i}\right)$$
$$= N_i E_i^\theta \ln(E_i). \qquad \text{(A2)}$$

The third equal sign of Eq. (A1) and the second of Eq. (A2) hold when

$$\frac{\epsilon_j^i - E_i}{E_i} \ll 1 \qquad \text{(A3)}$$

which is the case for the intervals other than the lowest ones. In Fig. 9, it is shown that those intervals account for only a very small probability, if the probabilities of the original system and pseudosystem have the forms

$$p_j^i = C n_j^i \left(\epsilon_j^i\right)^\theta e^{-\epsilon_j^i \beta}, \qquad \text{(A4)}$$

$$\hat{P}_i = C N_i (E_i)^\theta e^{-E_i \beta}. \qquad \text{(A5)}$$

For the properties of each interval of a given subspace (subsystem),

$$P_i = \sum_j p_j^i = C \sum_j n_j^i \left(\epsilon_j^i\right)^\theta e^{-\epsilon_j^i \beta}$$
$$= C \sum_j n_j^i \left(\epsilon_j^i\right)^\theta e^{-E_i \beta} e^{-(\epsilon_j^i - E_i)\beta} = C \sum_j n_j^i \left(\epsilon_j^i\right)^\theta e^{-E_i \beta}$$
$$= C e^{-E_i \beta} \sum_j n_j^i \left(\epsilon_j^i\right)^\theta = C N_i E_i^\theta e^{-E_i \beta} = \hat{P}_i, \qquad \text{(A6)}$$

$$\langle e \rangle_i = \sum_j p_j^i \epsilon_j^i = C \sum_j n_j^i \left(\epsilon_j^i\right)^{\theta+1} e^{-\epsilon_j^i \beta}$$
$$= C \sum_j n_j^i \left(\epsilon_j^i\right)^{\theta+1} e^{-E_i \beta} e^{-(\epsilon_j^i - E_i)\beta}$$
$$= C \sum_j n_j^i \left(\epsilon_j^i\right)^{\theta+1} e^{-E_i \beta} = C e^{-E_i \beta} \sum_j n_j^i \left(\epsilon_j^i\right)^{\theta+1}$$
$$= C N_i E_i^{\theta+1} e^{-E_i \beta} = \langle \hat{e} \rangle_i, \qquad \text{(A7)}$$

$$\langle s \rangle_i = -\sum_j p_j^i \ln \frac{p_j^i}{n_j^i} = -\beta \langle e \rangle_i + P_i \ln C - \sum_j p_j^i \theta \ln\left(\epsilon_j^i\right)$$
$$= \beta \langle e \rangle_i + P_i \ln C - P_i \theta \ln(E_i) = \langle \hat{s} \rangle_i. \qquad \text{(A8)}$$

The fourth equal sign in Eqs. (A6) and (A7) results from the quasicontinuous condition given by

$$\frac{1}{\beta} \gg |E_{i+1} - E_i| > \left|\epsilon_j^i - E_i\right|, \qquad \text{(A9)}$$

$$e^{-(\epsilon_j^i - E_i)\beta} \doteq 1. \qquad \text{(A10)}$$

In addition, under the quasicontinuous condition and the assumption that the probability distribution p_j^i or the distribution P_i or $\hat{P}_i$ have the property of higher order moment convergence at least to the second order in energy (e.g., as for the case of an ideal gas), the summation of discrete energy eigenlevels can be approximated by an integral over a continuous spectrum. Thus, properties for a given subsystem are found

from

$$\begin{aligned}\langle es\rangle_K &= \sum_i \sum_j p_j^i \epsilon_j^i \ln \frac{p_j^i}{n_j^i} \\ &= \sum_i \sum_j n_j^i \epsilon_j^i e^{-\beta\epsilon_j^i}\left[-\beta\epsilon_j^i + \ln C - \theta \ln\left(\epsilon_j^i\right)\right] \\ &= C\int n(E)E[-\beta E + \ln C - \theta \ln(E)]e^{-\beta E}dE,\end{aligned} \tag{A11}$$

$$\begin{aligned}\langle \hat{es}\rangle_K &= \sum_i \hat{P}_i E_i \ln \frac{\hat{P}_i}{N_i} \\ &= \sum_i N_i E_i e^{-\beta E_i}[-\beta E_i + \ln C - \theta \ln(E_i)] \\ &= C\int n(E)E[-\beta E + \ln C - \theta \ln(E)]e^{-\beta E}dE \\ &= \langle es\rangle_K,\end{aligned} \tag{A12}$$

$$\begin{aligned}\langle e^2\rangle_K &= \sum_i \sum_j p_j^i \left(\epsilon_j^i\right)^2 = \int E^2 p(E)dE \\ &= C\int n(E)E^{\theta+2}e^{-\beta E}dE,\end{aligned} \tag{A13}$$

$$\begin{aligned}\langle \hat{e^2}\rangle_K &= \sum_i \sum_j \hat{P}_i (E_i)^2 = \int E^2 p(E)dE \\ &= C\int n(E)E^{\theta+2}e^{-\beta E}dE = \langle e^2\rangle_K.\end{aligned} \tag{A14}$$

Note that both discrete summations of the original system and the pseudosystem can be regarded as the Riemann summation of the integral, and the difference of the Riemann summation and the integral is of second order or greater for the energy interval. This means that the difference between both Riemann summations (original system and pseudosystem) is of second order or greater when the quasicontinuous conditions hold. The properties for the system as a whole are then given by

$$\langle e\rangle = \sum_K^M \left(\sum_i \langle e\rangle_i\right)_K, \quad \langle \hat{e}\rangle = \sum_K^M \left(\sum_i \langle \hat{e}\rangle_i\right)_K, \tag{A15}$$

$$\langle s\rangle = \sum_K^M \left(\sum_i \langle s\rangle_i\right)_K, \quad \langle \hat{s}\rangle = \sum_K^M \left(\sum_i \langle \hat{s}\rangle_i\right)_K, \tag{A16}$$

$$\langle es\rangle = \sum_K^M \langle es\rangle_K, \quad \langle \hat{es}\rangle = \sum_K^M \langle \hat{es}\rangle_K, \tag{A17}$$

$$\langle e^2\rangle = \sum_K^M \langle e^2\rangle_K, \quad \langle \hat{e^2}\rangle = \sum_K^M \langle \hat{e^2}\rangle_K, \tag{A18}$$

where the summation is over all subsystems. With these expressions and the proof above linking the original and pseudosubsystem properties, it is also clear that $\langle \hat{A}_1\rangle$, $\langle \hat{A}_2\rangle$, and $\langle \hat{A}_3\rangle$ are equal to $\langle A_1\rangle$, $\langle A_2\rangle$, and $\langle A_3\rangle$ under the quasicontinuous condition. Thus, the solution of the equation of motion for the pseudosystem [Eq. (71)] can be used as a numerical approximation of that for the original system Eq. (70).

APPENDIX B: ONSAGER INVESTIGATION

Some results of the Onsager investigation using the concepts of hypoequilibrium state and nonequilibrium intensive properties found in Refs. [27,28] are given in the following. For a general discussion of the Onsager relations in SEAQT using the language of quantum mechanics, the reader is referred to [25]. If the system is in an Mth-order hypoequilibrium state, the probability evolution yields Eq. (32). For simplicity, the following definition is made:

$$\alpha^K = \ln Z^K - \ln p^K. \tag{B1}$$

Thus, the probability evolution of one energy eigenlevel is given by

$$\begin{aligned}p_i^K(t) &= \frac{p^K(t)}{Z^K[\beta^K(t)]} n_i^K e^{-\beta^K(t)\epsilon_i^K} \\ &= n_i^K e^{-\alpha^K(t)-\beta^K(t)\epsilon_i^K}.\end{aligned} \tag{B2}$$

α^K and β^K are nonequilibrium intensive properties in the Kth subspace, corresponding to the extensive properties of p^K and E^K. Furthermore, by defining

$$\alpha = \frac{A_2}{A_1}, \quad \beta = -\frac{A_3}{A_1} \tag{B3}$$

the particle number and energy evolution of the Kth subspace can be acquired from Eq. (36) by summation over one subspace, i.e.,

$$\frac{dp^K}{dt} = \frac{1}{\tau}p^K(\alpha^K - \alpha) + \frac{1}{\tau}E^K(\beta^K - \beta), \tag{B4}$$

$$\frac{dE^K}{dt} = \frac{1}{\tau}E^K(\alpha^K - \alpha) + \frac{1}{\tau}\langle e^2\rangle^K(\beta^K - \beta), \tag{B5}$$

where $\langle e^2\rangle^K$ is defined by Eq. (61) and p^K and E^K are the probability and energy in the Kth subspace. When a system is in an Mth-order hypoequilibrium state and goes through a pure relaxation process, a relation for the evolution of extensive properties evolution in one subspace exists and is expressed as

$$\frac{dS^K}{dt} = \beta^K \frac{dE^K}{dt} + (\alpha^K - 1)\frac{dp^K}{dt}, \tag{B6}$$

where S^K is the entropy in the Kth subspace. This is the Gibbs relation for the subspace. The physical meaning of β^K and α^K is then given by

$$\beta^K = \left(\frac{\partial S^K}{\partial E^K}\right)_{p^K} = \frac{1}{T^k}, \tag{B7}$$

$$\alpha^K - 1 = \left(\frac{\partial S^K}{\partial p^K}\right)_{E^K} = -\frac{\mu^K}{T^k}, \quad \mu^K = \left(\frac{\partial E^K}{\partial p^K}\right)_{S^K}, \tag{B8}$$

where T^K is the subspace temperature and μ^K is its chemical potential with respect to the subspace probability p^K. The differential change in the total entropy, which for a pure relaxation process is equivalent to the entropy generation, is then written as

$$\begin{aligned}dS &= \sum_K dS^K = \sum_K \beta^K dE^K + \sum_K (\alpha^K - 1)dp^K \\ &= \sum_K (\beta^K - \beta)dE^K + \sum_K (\alpha^K - \alpha)dp^K,\end{aligned} \tag{B9}$$

where both energy ($\sum dE^K = 0$) and probability ($\sum dp^K = 0$) conservation have been applied. The Casimir condition holds and $J_E^K = dE^K/dt$ and $J_p^K = dp^K/dt$ are defined to be the internal fluxes of energy and probability inside the system, while $X_p^K = \beta^K - \beta$ and $X_E^K = \alpha^K - \alpha$ are the conjugate forces. Thus,

$$\frac{dS}{dt} = \sum_K X_E^K J_E^K + \sum_K X_p^K J_p^K. \tag{B10}$$

The Onsager relations are acquired from Eqs. (B4) and (B5) in the form of $\mathbf{J} = \Lambda\mathbf{X}$, where Λ is symmetric and positive definite, so that

$$J_p^K = \frac{1}{\tau} p^K X_p^K + \frac{1}{\tau} E^K X_E^K, \tag{B11}$$

$$J_E^K = \frac{1}{\tau} E^K X_p^K + \frac{1}{\tau} \langle e^2 \rangle^K X_E^K, \tag{B12}$$

while the quadratic dissipation potential in force representation [30,31] is given by

$$\Xi(\mathbf{X},\mathbf{X}) = \frac{1}{2}\langle \mathbf{X}, \Lambda\mathbf{X}\rangle = \frac{1}{2\tau}\sum_K [p^K(\alpha^K - \alpha)^2 + 2E^K(\alpha^K - \alpha)(\beta^K - \beta) + \langle e^2\rangle^K(\beta^K - \beta)^2]. \tag{B13}$$

Furthermore, even though the following constraints apply to the fluxes

$$\sum_K J_p^K = 0, \quad \sum_K J_E^K = 0, \tag{B14}$$

the reciprocity seen in Eqs. (B11)–(B13) is fully consistent with the Onsager theory since according to Gyarmati [30] *the validity of Onsager's reciprocal relations is not influenced by a linear homogeneous dependence valid amongst the fluxes*. Thus, the physical interpretation of Eqs. (B11)–(B13) in terms of hypoequilibrium state and nonequilibrium intensive properties does not require a reformulation in terms of independent fluxes even though this could be done.

Thus, from the entropy generation of a nonequilibrium isolated system derived from the relaxation gradient dynamics, which are based on the geometry of system state space, one is able to arrive at the Onsager relations and the quadratic dissipation potential using the concepts of hypoequilibrium state and nonequilibrium intensive properties. Alternatively, one can arrive at these relations and this potential using a variational principle in system state space as is done in Ref. [25]. Of course, the Onsager relations and quadratic dissipation potential also correspond to a variational principle in the space spanned by conjugate forces and fluxes [30].

[1] M. Grmela and H. C. Öttinger, Dynamics and thermodynamics of complex fluids. I. Development of a general formalism, Phys. Rev. E **56**, 6620 (1997).

[2] H. C. Öttinger and M. Grmela, Dynamics and thermodynamics of complex fluids. II. Illustrations of a general formalism, Phys. Rev. E **56**, 6633 (1997).

[3] E. Weinan, *Principles of Multiscale Modeling* (Cambridge University Press, Cambridge, UK, 2011).

[4] K. Mohamed and A. Mohamad, A review of the development of hybrid atomistic–continuum methods for dense fluids, Microfluid. Nanofluid. **8**, 283 (2010).

[5] M. Kalweit and D. Drikakis, Multiscale simulation strategies and mesoscale modelling of gas and liquid flows, IMA J. Appl. Math. **76**, 661 (2011).

[6] G. P. Beretta, Steepest entropy ascent model for far-nonequilibrium thermodynamics: Unified implementation of the maximum entropy production principle, Phys. Rev. E **90**, 042113 (2014).

[7] H. C. Öttinger, *Beyond Equilibrium Thermodynamics* (Wiley, Hoboken, NJ, 2005).

[8] G. P. Beretta, E. P. Gyftopoulos, J. L. Park, and G. N. Hatsopoulos, Quantum thermodynamics. A new equation of motion for a single constituent of matter, Nuovo Cimento B, Ser. 11 **82**, 169 (1984).

[9] G. P. Beretta, E. P. Gyftopoulos, and J. L. Park, Quantum thermodynamics. A new equation of motion for a general quantum system, Nuovo Cimento B, Ser. 11 **87**, 77 (1985).

[10] G. P. Beretta, Nonlinear model dynamics for closed-system, constrained, maximal-entropy-generation relaxation by energy redistribution, Phys. Rev. E **73**, 026113 (2006).

[11] G. P. Beretta, Maximum entropy production rate in quantum thermodynamics, J. Phys.: Conf. Ser. **237**, 012004 (2010).

[12] G. P. Beretta, On the general equation of motion of quantum thermodynamics and the distinction between quantal and non-quantal uncertainties, arXiv:quant-ph/0509116.

[13] L. M. Martyushev and V. Seleznev, Maximum entropy production principle in physics, chemistry and biology, Phys. Rep. **426**, 1 (2006).

[14] E. P. Gyftopoulos and E. Çubukçu, Entropy: Thermodynamic definition and quantum expression, Phys. Rev. E **55**, 3851 (1997).

[15] E. Zanchini and G. P. Beretta, Recent progress in the definition of thermodynamic entropy, Entropy **16**, 1547 (2014).

[16] A. Montefusco, F. Consonni, and G. P. Beretta, Essential equivalence of the general equation for the nonequilibrium reversible-irreversible coupling (GENERIC) and steepest-entropy-ascent models of dissipation for nonequilibrium thermodynamics, Phys. Rev. E **91**, 042138 (2015).

[17] M. Grmela, Contact geometry of mesoscopic thermodynamics and dynamics, Entropy **16**, 1652 (2014).

[18] G. Li, O. Al-Abbasi, and M. R. von Spakovsky, Atomistic-level non-equilibrium model for chemically reactive systems based on steepest-entropy-ascent quantum thermodynamics, J. Phys.: Conf. Ser. **538**, 012013 (2014).

[19] S. Cano-Andrade, M. R. von Spakovsky, and G. P. Beretta, Steepest-Entropy-Ascent Quantum Thermodynamic Non-equilibrium Modeling of Decoherence of a Composite System of Two Interacting Spin-1/2 Systems, in *ASME 2013 International Mechanical Engineering Congress and Exposition* (American Society of Mechanical Engineers, New York, 2013), p. V08BT09A043.

[20] S. Cano-Andrade, G. P. Beretta, and M. R. von Spakovsky, Non-Equilibrium Thermodynamic Modeling of an Atom-Field State

Evolution with Comparisons to Published Experimental Data, in *Proceedings of the 12th Joint European Thermodynamics Conference, Brescia, Italy*, edited by M. Pilotelli and G. P. Beretta (Cartolibreria Snoopy, Brescia, Italy, 2013), pp. 1–5.

[21] S. Cano-Andrade, G. P. Beretta, and M. R. von Spakovsky, Steepest-entropy-ascent quantum thermodynamic modeling of decoherence in two different microscopic composite systems, Phys. Rev. A **91**, 013848 (2015).

[22] M. R. von Spakovsky and J. Gemmer, Some trends in quantum thermodynamics, Entropy **16**, 3434 (2014).

[23] C. E. Smith and M. R. von Spakovsky, Comparison of the non-equilibrium predictions of Intrinsic Quantum Thermodynamics at the atomistic level with experimental evidence, J. Phys.: Conf. Ser. **380**, 012015 (2012).

[24] G. P. Beretta and N. G. Hadjiconstantinou, Steepest Entropy Ascent Models of the Boltzmann Equation: Comparisons With Hard-Sphere Dynamics and Relaxation-Time Models for Homogeneous Relaxation From Highly Non-Equilibrium States, in *ASME 2013 International Mechanical Engineering Congress and Exposition* (American Society of Mechanical Engineers, New York, 2013), p. V08BT09A050.

[25] G. P. Beretta, Nonlinear quantum evolution equations to model irreversible adiabatic relaxation with maximal entropy production and other nonunitary processes, Rep. Math. Phys. **64**, 139 (2009).

[26] W. K. Wootters, Statistical distance and Hilbert space, Phys. Rev. D **23**, 357 (1981).

[27] G. Li and M. R. von Spakovsky, Steepest-entropy-ascent quantum thermodynamic modeling of heat and mass diffusion in a far-from-equilibrium system based on a single particle ensemble, arXiv:1601.01344.

[28] G. Li and M. R. von Spakovsky, Steepest-entropy-ascent quantum thermodynamic modeling of the far-from-equilibrium interactions between nonequilibrium systems of indistinguishable particle ensembles, arXiv:1601.02703.

[29] G. Li and M. R. von Spakovsky, Application of Steepest-Entropy-Ascent Quantum Thermodynamics to Predicting Heat and Mass Diffusion From the Atomistic Up to the Macroscopic Level, in *ASME 2015 International Mechanical Engineering Congress and Exposition* (American Society of Mechanical Engineers, New York, 2015), p. IMECE2015-53581.

[30] I. Gyarmati, E. Gyarmati, and W. F. Heinz, *Non-equilibrium Thermodynamics* (Springer, New York, 1970).

[31] M. Grmela, V. Klika, and M. Pavelka, Reductions and extensions in mesoscopic dynamics, Phys. Rev. E **92**, 032111 (2015).

[32] G. P. Beretta and M. R. von Spakovsky, Steepest-entropy-ascent quantum thermodynamic framework for describing the non-equilibrium behavior of a chemically reactive system at an atomistic level, arXiv:1504.03994.

[33] G. Li and M. R. von Spakovsky, Study of the Transient Behavior and Microstructure Degradation of a SOFC Cathode Using an Oxygen Reduction Model Based on Steepest-Entropy-Ascent Quantum Thermodynamics, in *ASME 2015 International Mechanical Engineering Congress and Exposition* (American Society of Mechanical Engineers, New York, 2015), p. IMECE2015-53726.

[34] G. Li and M. R. von Spakovsky, Multiscale transient and steady state study of the influence of microstructure degradation and chromium oxide poisoning on SOFC cathode performance (unpublished).

[35] M. Grmela, Fluctuations in extended mass-action-law dynamics, Physica D (Amsterdam) **241**, 976 (2012).

[36] E. P. Gyftopoulos and G. P. Beretta, *Thermodynamics: Foundations and Applications* (Dover, New York, 2005).